Hunting for extremely metal-poor emission-line galaxies in the Sloan Digital Sky Survey: MMT and 3.5 m APO observations

Y. I. Izotov, T. X. Thuan, N. G. Guseva

A&A 546, A122 (2012)
DOI: 10.1051/0004-6361/201219733

Astronomy & Astrophysics

Hunting for extremely metal-poor emission-line galaxies in the Sloan Digital Sky Survey: MMT and 3.5 m APO observations⋆,⋆⋆

Y. I. Izotov[1,2], T. X. Thuan[3,4], and N. G. Guseva[1,2]

[1] Max-Planck-Institut für Radioastronomie, Auf dem Hügel 69, 53121 Bonn, Germany
[2] Main Astronomical Observatory, Ukrainian National Academy of Sciences, Zabolotnoho 27, Kyiv 03680, Ukraine
e-mail: izotov@mao.kiev.ua
[3] Institut d'Astrophysique de Paris, 98bis boulevard Arago, 75014 Paris, France
[4] Astronomy Department, University of Virginia, PO Box 400325, Charlottesville, VA 22904, USA

Received 1 June 2012 / Accepted 24 July 2012

ABSTRACT

We present 6.5-m MMT and 3.5 m APO spectrophotometry of 69 H II regions in 42 low-metallicity emission-line galaxies, selected from the data release 7 of the Sloan Digital Sky Survey to have mostly [O III]λ4959/H$\beta \lesssim 1$ and [N II]λ6583/H$\beta \lesssim 0.1$. The electron temperature-sensitive emission line [O III] λ4363 is detected in 53 H II regions allowing a direct abundance determination. The oxygen abundance in the remaining 16 H II regions is derived using a semi-empirical method. The oxygen abundance of the galaxies in our sample ranges from 12 + log O/H ~ 7.1 to ~7.9, with 14 H II regions in 7 galaxies with 12 + log O/H $\leq$ 7.35. In 5 of the latter galaxies, the oxygen abundance is derived here for the first time. Including other known extremely metal-deficient emission-line galaxies from the literature, e.g. SBS 0335−052W, SBS 0335−052E and I Zw 18, we have compiled a sample of the 17 most metal-deficient (with 12 + log O/H $\leq$ 7.35) emission-line galaxies known in the local universe. There appears to be a metallicity floor at 12 + log O/H ~ 6.9, suggesting that the matter from which dwarf emission-line galaxies formed was pre-enriched to that level by e.g. Population III stars.

Key words. galaxies: abundances – galaxies: irregular – galaxies: evolution – galaxies: ISM – HII regions – ISM: abundances

1. Introduction

Extremely metal-deficient (XMD) emission-line galaxies at low redshifts are the most promising young galaxy candidates in the local Universe (Guseva et al. 2003; Izotov & Thuan 2004b). Those XMD objects are often defined as emission-line galaxies with an oxygen abundance 12 + log O/H $\leq$ 7.65 (e.g. Kniazev et al. 2003; Kakazu et al. 2007; Pustilnik & Martin 2007; Ekta & Chengalur 2010), a definition which we will adopt hereafter. These galaxies are important to identify because of several reasons. First, their nearly pristine interstellar medium (ISM) can shed light on the properties of the primordial ISM at the time of galaxy formation. There is now some evidence of a metallicity floor, i.e. that even the most metal-deficient star-forming galaxies in the local Universe formed from matter which was already pre-enriched by a previous star formation episode, e.g. by Population III stars (Thuan et al. 2005). A similar metallicity floor appears also to be present in damped Lyα systems (Prochaska et al. 2003). It is thus quite important to find as many emission-line XMD galaxies as possible, especially the ones with the lowest metallicities, to have enough statistics to assess the reality of such a metallicity floor, and in so doing, to establish firmly the level of that pre-enrichment. Second, because they have not undergone much chemical evolution, these galaxies are also the best objects for the determination of the primordial ^{4}He abundance Y_p (e.g. Izotov & Thuan 2004a; Izotov et al. 2007). A recent determination of Y_p (Izotov & Thuan 2010) appears to indicate that a small deviation from the standard Big Bang nucleosynthesis model may exist, suggesting new physics such as the existence of light sterile neutrinos. It is important to confirm this result by improving the determination of Y_p with as many XMD emission-line galaxies as possible. Third, in the hierarchical picture of galaxy formation, large galaxies form from the assembly of small dwarf galaxies. While much progress has been made in finding large populations of galaxies at high redshifts ($z \gtrsim 3$, Steidel et al. 2003), truly young galaxies in the process of forming remain elusive in the distant universe. The spectra of those far-away galaxies generally show the presence of a substantial amount of heavy elements, indicating previous star formation and metal enrichment. Therefore, XMD emission-line dwarf galaxies are possibly the closest approximations we can find of the elementary primordial units from which galaxies formed. Their relative proximity allows studies of their stellar, gas and dust content with a sensitivity, spectral and spatial resolution that faint distant high-redshift galaxies do not allow.

XMD emission-line galaxies are however very rare (e.g. Kunth & Östlin 2000). Many surveys have been carried out to search for such galaxies without significant success. For more than three decades, one of the first blue compact dwarf (BCD)

⋆ Based on observations with the Multiple Mirror telescope (MMT) and the 3.5 m Apache Point Observatory (APO). The MMT is operated by the MMT Observatory (MMTO), a joint venture of the Smithsonian Institution and the University of Arizona. The Apache Point Observatory 3.5-m telescope is owned and operated by the Astrophysical Research Consortium.

⋆⋆ Figures 1–3 and Tables 2–8 are available in electronic form at http://www.aanda.org

galaxies discovered, I Zw 18 (Sargent & Searle 1970), continued to hold the record as the most metal-deficient emission-line galaxy known, with an oxygen abundance $12 + \log \mathrm{O/H} = 7.17 \pm 0.01$ in its northwestern component and 7.22 ± 0.02 in its southeastern component (Thuan & Izotov 2005). Only very recently, has I Zw 18 been displaced by the BCD SBS 0335–052W which was discovered by Pustilnik et al. (1997). This galaxy, with an oxygen abundance $12+\log \mathrm{O/H} = 7.12 \pm 0.03$, is now the emission-line galaxy with the lowest metallicity known (Izotov et al. 2005). Recently, Izotov et al. (2009) derived the oxygen abundance in four H II regions of SBS 0335–052W and found that it varies from region to region in the range 6.86–7.22.

Because of the scarcity of XMD emission-line galaxies such as I Zw 18 and SBS 0335–052W, we stand a better chance of finding them in very large spectroscopic surveys. One of the best surveys suitable for such a search is the Sloan Digital Sky Survey (SDSS; York et al. 2000). However, despite intensive studies of galaxies with a detected temperature-sensitive [O III] λ4363 emission line in their spectra, no emission-line galaxy with an oxygen abundance as low as that of I Zw 18 has been discovered in the SDSS data release 3 (DR3) and earlier releases. The lowest-metallicity emission-line galaxies found in these releases have oxygen abundances $12 + \log \mathrm{O/H} > 7.4$ (Kniazev et al. 2003, 2004; Izotov et al. 2004, 2006a). Only recently, have Pustilnik et al. (2005), Izotov et al. (2006b), Izotov & Thuan (2007, 2009) and Guseva et al. (2007) found several galaxies with $12 + \log \mathrm{O/H} \leq 7.35$ in later SDSS spectroscopic releases.

In order to find new candidates for XMD emission-line galaxies, we have carried out a systematic search for such objects in the SDSS data release 7 (DR7). We have chosen them mainly on the basis of the relative fluxes of selected emission lines, as described in Izotov et al. (2006b) and Izotov & Thuan (2007). All known XMD emission-line galaxies are characterised by relatively weak (compared to Hβ) [O II] λ3727, [O III] λ4959, λ5007 and [N II] λ6583 emission lines (e.g. Izotov & Thuan 1998a,b; Izotov et al. 2005; Pustilnik et al. 2005; Izotov et al. 2006b). These spectral properties select out uniquely low-metallicity dwarfs since no other type of galaxy possesses them. This technique appears to be more efficient in uncovering XMD galaxies with the lowest metallicities, those with $12+\log \mathrm{O/H} \leq 7.35$, as compared to the selection technique based on broad-band photometric colors used e.g. by Brown et al. (2008) who found only objects with $12+\log \mathrm{O/H} > 7.35$. In contrast to previous studies (Kniazev et al. 2003, 2004; Izotov et al. 2004, 2006a) which focus exclusively on objects with a detected [O III] λ4363 emission line in the SDSS sprectra, we have also considered objects which satisfy the criteria described above, but with spectra where [O III] λ4363 is weak or not detected. Since the [O II] λ3727 line is out of the observed wavelength range in SDSS spectra of galaxies with a redshift z lower than 0.02, we use the two following criteria to select candidate XMD emission-line galaxies: [O III]λ4959/H$\beta \lesssim 1$ and [N II]λ6583/H$\beta \lesssim 0.1$. The efficiency of this technique to achieve our goals has been demonstrated by Izotov et al. (2006b) and Izotov & Thuan (2007).

While the SDSS spectra allow us to select very low metallicity galaxies, we need additional spectral observations for the following reasons: 1) spectra that go further into the blue wavelength range than SDSS spectra are required to detect the [O II] λ3727 line. For a precise oxygen abundance determination, this line is needed to provide information on the singly ionised ionic population of oxygen. In principle, the [O II] λ7320, 7330 emission lines can be used instead. However, these lines are very weak or not detected in the SDSS spectra of low-metallicity candidates; 2) a better signal-to-noise ratio spectrum may allow the detection of a weak [O III] λ4363 emission line, which would permit a direct determination of the electron temperature; 3) very often, low-metallicity candidates possess two or more H II regions with different degrees of excitation. However, SDSS spectra are usually obtained for only one H II region, chosen sometimes not in the most optimal way.

For these reasons, we have obtained new spectroscopic observations with the 3.5 m APO telescope and the MMT of a sample of SDSS XMD emission-line galaxy candidates. In addition to the galaxies selected by using the criteria described above, we have also selected a subsample of low-redshift ($z < 0.02$) SDSS galaxies with high excitation ([O III]λ4959/H$\beta > 1$) to improve their abundance determination with MMT/Blue channel observations, because their [O II]λ3727 emission line is not included in the spectral range of their SDSS spectra. The motivation for observing this subsample is the fact that XMD BCDs like I Zw 18 and SBS 0335−052 are also often characterised by high excitation. The observations and data reduction are discussed in Sect. 2. The element abundances are derived in Sect. 3. We consider in Sect. 4 the luminosity−metallicity relations for XMD emission-line galaxies and the issue of a metallicity floor, and in Sect. 5 their location in the emission-line diagnostic diagram. Our main findings are summarised in Sect. 6.

2. Observations and data reduction

2.1. APO observations

New optical spectra were obtained for a subsample of galaxies using the 3.5 m APO telescope in the course of several nights during the February 2008–February 2009 period. The general characteristics of these galaxies, such as redshift, distance, apparent B magnitude (if available in the literature) or SDSS g magnitude and other names are shown in Table 1. The Journal of observations is shown in Table 2. The 3.5 m APO observations were made with the Dual Imaging Spectrograph (DIS) in the both the blue and red wavelength ranges. In the blue range, we use the B400 grating with a linear dispersion of 1.83 Å/pix and a central wavelength of 4400 Å, while in the red range we use the R300 grating with a linear dispersion 2.31 Å/pix and a central wavelength of 7500 Å. The above instrumental set-up gave a spatial scale along the slit of 0.″4 pixel^{-1}, a spectral range ~3600–9600 Å and a spectral resolution of 7 Å (*FWHM*). The slit orientation, the total exposure time and the airmass during observations are shown in Table 2. Several Kitt Peak IRS spectroscopic standard stars were observed for flux calibration. Spectra of He-Ne-Ar comparison arcs were obtained at the beginning or the end of each night for wavelength calibration.

2.2. MMT observations

The MMT spectrophotometric observations were obtained on the nights of 2008 March 28–29, and 2010 April 13. The galaxies are listed in Table 1 separately for low- and medium- spectral resolution observations. All observations have been made with the Blue Channel of the MMT spectrograph. The log of the observations is given in Table 2. We used a 300 grooves/mm grating in first order for the low-resolution observations and a 800 grooves/mm grating in first order for the medium-resolution observations. The above instrumental set-ups gave a spatial scale along the slit of 0.″6 pixel^{-1}, and respectively a spectral range of 3600−7500 Å and a spectral resolution of ~7 Å (*FWHM*)

Table 1. General characteristics of galaxies.

Name	RA(J2000.0)	Dec(J2000.0)	Redshift	Distance Mpc	B, g	Other names	Reference[a]
a) 3.5 m APO observations							
J0113+0052No.1	01:13:40.45	+00:52:39.14	0.00383	15.80	13.69 ± 0.01	UGC 772	2
J0113+0052No.2	01:13:40.45	+00:52:39.14	0.00383	15.80	13.69 ± 0.01	UGC 772	2
J0113+0052No.3	01:13:40.45	+00:52:39.14	0.00383	15.80	13.69 ± 0.01	UGC 772	2
J0113+0052No.4	01:13:40.45	+00:52:39.14	0.00383	15.80	13.69 ± 0.01	UGC 772	2
J0138+0020	01:38:35.02	+00:20:05.12	0.01696	67.84	19.14 ± 0.02		1
J0834+5905No.1	08:34:37.19	+59:05:35.99	0.00477	19.08	19.87 ± 0.02		1
J0834+5905No.2	08:34:37.19	+59:05:35.99	0.00477	19.08	19.87 ± 0.02		1
J0843+4025	08:43:37.99	+40:25:46.96	0.00205	10.17	17.57 ± 0.02		1
J0851+8416	08:51:03.55	+84:16:13.33	0.00614	29.70	16.00 ± 0.01	UGC 4557	1
J0906+2528No.1	09:06:00.92	+25:28:11.33	0.00921	39.50	17.41 ± 0.01		1
J0906+2528No.2	09:06:00.92	+25:28:11.33	0.00921	39.50	17.41 ± 0.01		1
J0908+0517No.1	09:08:36.53	+05:17:26.95	0.00202	6.45	16.96 ± 0.24	KKH 46	3
J0908+0517No.2	09:08:36.53	+05:17:26.95	0.00208	6.45	16.96 ± 0.24	KKH 46	3
J0950+3127No.1	09:50:19.49	+31:27:22.24	0.00203	7.25	15.41 ± 0.01	UGC 5272b	4
J0950+3127No.2	09:50:19.49	+31:27:22.24	0.00201	7.25	15.41 ± 0.01	UGC 5272b	4
DDO68 No.2	09:56:46.05	+28:49:43.78	0.00203	5.85	14.30 ± 0.00	UGC 534, J0956+2849No.2	5
DDO68 No.3	09:56:46.05	+28:49:43.78	0.00196	5.85	14.30 ± 0.00	UGC 534, J0956+2849No.3	5
J1056+3608No.1	10:56:40.35	+36:08:27.94	0.00218	7.68	18.54 ± 0.02	HS 1053+3624	1
J1056+3608No.2	10:56:40.35	+36:08:27.94	0.00200	7.68	18.54 ± 0.02	HS 1053+3624	1
J1056+3608No.3	10:56:40.35	+36:08:27.94	0.00206	7.68	18.54 ± 0.02	HS 1053+3624	1
J1109+2007	11:09:09.53	+20:07:29.75	0.00373	14.92	17.20 ± 0.01		1
J1119+0935No.1	11:19:28.09	+09:35:44.28	0.00317	12.10	16.42 ± 0.01		1
J1119+0935No.2	11:19:28.09	+09:35:44.28	0.00343	12.10	16.42 ± 0.01		1
J1119+0935No.3	11:19:28.09	+09:35:44.28	0.00340	12.10	16.42 ± 0.01		1
J1121+3744No.1	11:21:46.68	+37:44:21.18	0.00679	31.00	17.87 ± 0.01		1
J1121+3744No.2	11:21:46.68	+37:44:21.18	0.00679	31.00	17.87 ± 0.01		1
J1146+4050	11:46:37.60	+40:50:36.68	0.00288	15.90	17.40 ± 0.01		1
J1226−0115No.1	12:26:22.70	−01:15:12.33	0.00659	30.80	16.26 ± 0.01	UM 501	6
J1226−0115No.2	12:26:22.70	−01:15:12.33	0.00659	30.80	16.26 ± 0.01	UM 501	6
J1235+2755No.1	12:35:52.35	+27:55:54.22	0.00291	11.64	16.72 ± 0.14		7
J1235+2755No.2	12:35:52.35	+27:55:54.22	0.00280	11.64	16.72 ± 0.14		7
J1235+2755No.3	12:35:52.35	+27:55:54.22	0.00280	11.64	16.72 ± 0.14		7
J1241−0340	12:41:59.35	−03:40:02.42	0.00944	40.10	18.07 ± 0.01		1
J1257+3341No.1	12:57:40.55	+33:41:39.24	0.00299	15.10	17.43 ± 0.01		1
J1257+3341No.2	12:57:40.55	+33:41:39.24	0.00307	15.10	17.43 ± 0.01		1
J1257+3341No.3	12:57:40.55	+33:41:39.24	0.00308	15.10	17.43 ± 0.01		1
J1403+5804No.1	14:03:21.46	+58:04:03.44	0.00237	14.26	17.12 ± 0.01		1
J1403+5804No.2	14:03:21.46	+58:04:03.44	0.00242	14.26	17.12 ± 0.01		1
SBS1420+544	14:22:38.80	+54:14:10.00	0.00242	88.90	17.70 ± 0.01	J1422+5414	1
PHL293B	22:30:36.79	−00:06:36.96	0.00583	24.40	16.98 ± 0.01	J2230−0006	1
b) low-resolution MMT observations							
J1016+3754	10:16:24.53	+37:54:45.97	0.00392	19.90	15.90 ± 0.01	HS 1013+3809	1
J1016+5823No.1	10:16:53.11	+58:23:40.33	0.00768	35.40	15.90 ± 0.20	UGC 5541	5
J1016+5823No.2	10:16:53.11	+58:23:40.33	0.00744	35.40	15.90 ± 0.20	UGC 5541	5
J1016+5823No.3	10:16:53.11	+58:23:40.33	0.00780	35.40	15.90 ± 0.20	UGC 5541	5
J1044+0353	10:44:57.80	+03:53:13.15	0.01296	54.50	17.48 ± 0.06		1
J1119+5130	11:19:34.32	+51:30:12.13	0.00473	23.10	16.94 ± 0.00	ARP'S GALAXY	
J1132+5722No.1	11:32:02.62	+57:22:36.56	0.00507	26.40	16.19 ± 0.01	SBS 1129+576	1
J1132+5722No.2	11:32:02.62	+57:22:36.56	0.00534	26.40	16.19 ± 0.01	SBS 1129+576	1
J1132+5722No.3	11:32:02.62	+57:22:36.56	0.00521	26.40	16.19 ± 0.01	SBS 1129+576	1
J1154+4636	11:54:41.22	+46:36:36.35	0.00360	19.30	17.21 ± 0.01	CG 1473	1
J1215+5223	12:15:46.62	+52:23:13.85	0.00046	3.33	15.17 ± 0.00	CGCG 269-049	1
J1224+3724	12:24:36.72	+37:24:36.55	0.04040	179.90	17.86 ± 0.01	CG 1022, HS 1222+3741	1
J1244+3212No.1	12:44:05.98	+32:12:32.33	0.00223	7.51	10.10 ± 0.01	NGC 4656	5
J1244+3212No.2	12:44:05.98	+32:12:32.33	0.00206	7.51	10.10 ± 0.01	NGC 4656	5
J1244+3212No.3	12:44:05.98	+32:12:32.33	0.00207	7.51	10.10 ± 0.01	NGC 4656	5
J1248+4823	12:48:27.79	+48:23:03.29	0.02955	124.60	18.09 ± 0.01	HS 1246+4839	1
J1327+4022	13:27:23.29	+40:22:04.15	0.01049	48.00	19.11 ± 0.01		1
J1331+4151	13:31:26.90	+41:51:48.29	0.01168	52.60	16.92 ± 0.00		1
J1355+4651	13:55:25.64	+46:51:51.34	0.02812	118.30	19.26 ± 0.01	HS 1353+4706	1
J1608+3528	16:08:10.36	+35:28:09.30	0.03241	138.90	18.75 ± 0.02		1

Notes. [a] References on the photometric data. The g magnitudes are from the SDSS and the B magnitudes are from other sources. The coding is as follows: (1) SDSS; (2) Patterson & Thuan (1996); (3) Makarova et al. (2009); (4) Karachentsev et al. (2004); (5) de Vaucouleurs et al. (1991); (6) Doyle et al. (2005); (7) Odewahn & Aldering (1995).

Table 1. continued.

Name	RA(J2000.0)	Dec(J2000.0)	Redshift	Distance Mpc	B, g	Other names	Reference[a]
c) medium-resolution MMT observations							
J0810+1837	08:10:30.66	+18:37:04.22	0.00657	21.70	17.97 ± 0.02		1
J0833+2508No.1	08:33:35.65	+25:08:47.14	0.00759	32.10	18.00 ± 0.01		1
J0833+2508No.2	08:33:35.65	+25:08:47.14	0.00759	32.10	18.00 ± 0.01		1
J0834+5905	08:34:37.19	+59:05:35.99	0.00477	19.08	19.87 ± 0.02		1
J0931+2717No.1	09:31:36.15	+27:17:46.64	0.00507	23.40	17.71 ± 0.01		1
J0931+2717No.2	09:31:36.15	+27:17:46.64	0.00507	23.40	17.71 ± 0.01		1
DDO68 No.3	09:56:46.05	+28:49:43.78	0.00188	5.85	14.30 ± 0.00	UGC 534, J0956+2849No.3	1
DDO68 No.4	09:56:46.05	+28:49:43.78	0.00185	5.85	14.30 ± 0.00	UGC 534, J0956+2849No.4	1
J0959+4626	09:59:05.76	+46:26:50.49	0.00200	8.00	17.80 ± 0.01		1
J1057+1358No.1	10:57:38.15	+13:58:44.53	0.00424	20.20	17.24 ± 0.02		1
J1057+1358No.2	10:57:38.15	+13:58:44.53	0.00424	20.20	17.24 ± 0.02		1
J1121+3744No.1	11:21:46.68	+37:44:21.18	0.00657	31.00	17.87 ± 0.01		1
J1121+3744No.2	11:21:46.68	+37:44:21.18	0.00657	31.00	17.87 ± 0.01		1
J1231+4205	12:31:09.08	+42:05:33.89	0.00190	8.19	17.78 ± 0.02		1

for the low-resolution observations, and of 3200–5200 Å and ∼3 Å (*FWHM*) for the medium-resolution ones. The total exposure times, orientations of the slit and airmasses for each MMT observation are given in Table 2. In 2008, the Kitt Peak IRS spectroscopic standard stars BD 33d2642 and HZ 44 were observed for flux calibration during the first night, while BD 33d2642, BD 75d325 and Feige 34 were observed during the second night. In 2010, BD 33d2642, BD 75d325 and Feige 34 were observed. Spectra of He-Ne-Ar comparison arcs were obtained before and after each observation to calibrate the wavelength scale.

2.3. Results

Several galaxies listed in Table 1 have been observed previously by other authors. To improve their abundance determination, we have reobserved J0113+0052, DDO 68, SBS 1116+517, SBS 1129+576, SBS 1420+544 and PHL 293B. Two galaxies, J1121+3744 and J0834+5905, were observed twice, both with the 3.5 m APO and the MMT.

The two-dimensional spectra were bias subtracted and flat-field corrected using IRAF[1]. We then use the IRAF software routines IDENTIFY, REIDENTIFY, FITCOORD, TRANSFORM to perform wavelength calibration and correct for distortion and tilt for each frame. One-dimensional spectra were then extracted from each frame using the APALL routine. The sensitivity curve was obtained by fitting with a high-order polynomial the observed spectral energy distribution of standard stars. Then sensitivity curves obtained from observations of different stars during the same night were averaged.

The 3.5 m APO, the low- and medium-resolution MMT H II region spectra are shown respectively in Figs. 1–3. These spectra have all been reduced to zero redshift.

The extinction-corrected line fluxes $I(\lambda)$, normalised to $I(\mathrm{H}\beta)$ and multiplied by a factor of 100, and their errors, derived from the 3.5 m APO, MMT low-resolution and MMT medium-resolution observations are given in Tables 3–5, respectively. The data were obtained using the IRAF SPLOT routine. The line flux errors listed include statistical errors derived with SPLOT from non-flux calibrated spectra, in addition to errors introduced in the standard star absolute flux calibration, which we set to 1% of the line fluxes. These errors will be later propagated into the calculation of abundance errors. The line fluxes were corrected for both reddening (using the extinction curve of Whitford 1958) and underlying hydrogen stellar absorption derived simultaneously by an iterative procedure as described in Izotov et al. (1994). The extinction coefficient is defined as $C(\mathrm{H}\beta) = 1.47E(B-V)$, where $E(B-V) = A(V)/3.2$ and $A(V)$ is the extinction in the V band (Aller 1984). Equivalent widths $EW(\mathrm{H}\beta)$, extinction coefficients $C(\mathrm{H}\beta)$, and equivalent widths EW(abs) of the hydrogen absorption stellar lines are also given in Tables 3–5, along with the uncorrected Hβ fluxes.

3. Physical conditions and element abundances

To determine element abundances, we generally follow the procedures of Izotov et al. (1994, 1997) and Thuan et al. (1995). We adopt a two-zone photoionised H II region model: a high-ionisation zone with temperature T_e(O III), where [O III] and [Ne III] lines originate, and a low-ionisation zone with temperature T_e(O II), where [O II], [N II] and [S II] lines originate. As for the [S III] and [Ar III] lines they originate in the intermediate zone between the high and low-ionisation regions. In the H II regions with a detected [O III] λ4363 emission line, the temperature T_e(O III) is calculated using the "direct" method based on the [O III] λ4363/(λ4959+λ5007) line ratio. In H II regions where the [O III] λ4363 emission line is not detected, we used a semi-empirical method described by Izotov & Thuan (2007) to derive T_e(O III).

For T_e(O II), we use the relation between the electron temperatures T_e(O III) and T_e(O II) obtained by Izotov et al. (2006a) from the H II photoionisation models of Stasińska & Izotov (2003). These are based on more recent stellar atmosphere models and improved atomic data as compared to the Stasińska (1990) models. Ionic and total heavy element abundances are derived using expressions for ionic abundances and ionisation correction factors obtained by Izotov et al. (2006a). The element abundances are given in Tables 6–8 along with the adopted electron temperatures for different ions.

Table 9 summarises the abundance determinations for all H II regions, where we show the oxygen abundance 12+log O/H, the logarithms of abundance ratios log N/O, log Ne/O, log S/O and log Ar/O, the extinction coefficient $C(\mathrm{H}\beta)$, the equivalent width of the Hβ emission line, and the galaxy's absolute

[1] IRAF is distributed by National Optical Astronomical Observatory, which is operated by the Association of Universities for Research in Astronomy, Inc., under cooperative agreement with the National Science Foundation.

Table 9. Abundances, extinction coefficients, Hβ equivalent widths, and absolute magnitudes.

Name	12 + log O/H[a]	log N/O	log Ne/O	log S/O	log Ar/O	C(Hβ)	EW(Hβ)	M_g, M_B
a) 3.5 m APO observations								
J0113+0052No.1	7.15 ± 0.09(D)	...	−0.72 ± 0.21	...	...	0.065	40.7	−17.62
J0113+0052No.2	7.32 ± 0.04(D)	−1.50 ± 0.08	...	...	...	0.035	20.8	−17.62
J0113+0052No.3	7.30 ± 0.08(D)	...	...	...	...	0.115	30.0	−17.62
J0113+0052No.4	7.32 ± 0.04(D)	−1.43 ± 0.07	...	...	...	0.045	47.3	−17.62
J0138+0020	7.52 ± 0.07(E)	...	...	...	...	0.210	20.4	−15.15
J0834+5905No.1	7.43 ± 0.05(E)	−1.49 ± 0.10	...	...	...	0.285	17.9	−12.03
J0834+5905No.2	7.37 ± 0.06(E)	...	...	...	...	0.135	9.9	−12.03
J0843+4025	7.57 ± 0.06(E)	−1.58 ± 0.10	...	...	...	0.000	16.3	−12.47
J0851+8416	7.66 ± 0.06(D)	−1.47 ± 0.09	−0.93 ± 0.14	...	...	0.135	83.6	−16.75
J0906+2528No.1	7.50 ± 0.14(D)	−1.77 ± 0.19	−0.93 ± 0.43	...	...	0.210	12.2	−16.22
J0906+2528No.2	7.46 ± 0.09(D)	−1.43 ± 0.12	−0.81 ± 0.22	...	...	0.240	37.1	−16.22
J0908+0517No.1	7.39 ± 0.08(E)	−1.46 ± 0.15	...	...	...	0.410	17.2	−12.73
J0908+0517No.2	7.68 ± 0.03(D)	−1.32 ± 0.04	−0.76 ± 0.05	−1.49 ± 0.06	−2.17 ± 0.04	0.040	197.4	−12.73
J0950+3127No.1	7.41 ± 0.07(E)	...	...	...	...	0.005	14.5	−14.10
J0950+3127No.2	7.45 ± 0.17(D)	−1.62 ± 0.25	...	...	−2.04 ± 0.22	0.140	124.6	−14.10
DDO68 No.2	7.18 ± 0.05(D)	...	−0.79 ± 0.10	...	−2.28 ± 0.07	0.030	191.6	−14.59
DDO68 No.3	7.08 ± 0.09(D)	...	−0.93 ± 0.22	...	...	0.005	85.3	−14.59
J1056+3608No.1	7.16 ± 0.07(D)	−1.45 ± 0.25	−0.83 ± 0.17	...	...	0.340	134.4	−11.21
J1056+3608No.2	7.32 ± 0.16(D)	−1.47 ± 0.22	...	...	...	0.000	31.7	−11.21
J1056+3608No.3	7.31 ± 0.11(D)	−1.46 ± 0.16	−0.70 ± 0.32	...	...	0.000	32.5	−11.21
J1109+2007	7.47 ± 0.10(D)	−1.77 ± 0.14	...	...	...	0.350	22.6	−14.67
J1119+0935No.1	7.47 ± 0.05(E)	−1.43 ± 0.09	...	...	−2.49 ± 0.13	0.055	18.7	−14.53
J1119+0935No.2	7.70 ± 0.06(D)	−1.49 ± 0.08	−0.87 ± 0.13	...	−2.47 ± 0.07	0.225	57.6	−14.53
J1119+0935No.3	7.43 ± 0.09(E)	−1.44 ± 0.17	...	...	...	0.280	29.5	−14.53
J1121+3744No.1	6.78 ± 0.16(E)	...	...	...	...	0.000	8.9	−14.59
J1146+4050	7.34 ± 0.06(E)	−1.31 ± 0.10	...	...	−2.21 ± 0.18	0.110	17.9	−13.92
J1226−0115No.1	7.77 ± 0.02(D)	−1.44 ± 0.02	−0.78 ± 0.03	−1.59 ± 0.03	−2.20 ± 0.03	0.130	158.5	−16.76
J1226−0115No.2	7.81 ± 0.02(D)	−1.37 ± 0.02	−0.83 ± 0.03	−1.55 ± 0.03	−2.27 ± 0.04	0.275	149.2	−16.76
J1235+2755No.1	7.58 ± 0.05(E)	−1.74 ± 0.07	−0.82 ± 0.14	...	...	0.105	36.7	−13.99
J1235+2755No.2	7.83 ± 0.02(D)	−1.51 ± 0.03	−0.76 ± 0.05	−1.78 ± 0.05	−2.42 ± 0.03	0.075	129.8	−13.99
J1235+2755No.3	7.77 ± 0.03(D)	−1.52 ± 0.04	−0.78 ± 0.07	−1.80 ± 0.05	−2.37 ± 0.04	0.220	156.6	−13.99
J1241−0340	7.74 ± 0.01(D)	−1.54 ± 0.02	−0.69 ± 0.03	−1.64 ± 0.03	−2.27 ± 0.02	0.310	125.3	−15.83
J1257+3341No.1	7.47 ± 0.11(D)	−1.44 ± 0.15	−0.83 ± 0.28	...	−2.51 ± 0.16	0.055	75.7	−13.52
J1257+3341No.2	7.62 ± 0.07(E)	...	−0.59 ± 0.21	...	...	0.000	22.8	−13.52
J1257+3341No.3	7.48 ± 0.09(D)	−1.53 ± 0.13	−0.88 ± 0.27	...	−2.45 ± 0.14	0.000	90.6	−13.52
J1403+5804No.1	7.36 ± 0.06(E)	−1.49 ± 0.12	...	...	...	0.070	9.1	−14.01
J1403+5804No.2	7.40 ± 0.05(D)	−1.64 ± 0.08	−0.79 ± 0.11	...	−2.37 ± 0.08	0.180	46.4	−14.01
SBS1420+544	7.79 ± 0.02(D)	−1.54 ± 0.03	−0.69 ± 0.03	−1.61 ± 0.05	−2.21 ± 0.06	0.105	201.8	−17.34
PHL293B	7.67 ± 0.02(D)	−1.80 ± 0.03	−0.70 ± 0.03	−1.78 ± 0.05	−2.40 ± 0.05	0.115	69.6	−15.29
b) low-resolution MMT observations								
J1016+3754	7.64 ± 0.01(D)	−1.55 ± 0.03	−0.76 ± 0.02	−1.52 ± 0.03	−2.26 ± 0.04	0.115	96.3	−15.92
J1016+5823No.1	7.74 ± 0.01(D)	−1.71 ± 0.02	−0.77 ± 0.02	−1.68 ± 0.04	−2.54 ± 0.03	0.000	125.8	−17.29
J1016+5823No.2	7.59 ± 0.06(D)	−1.43 ± 0.08	−0.88 ± 0.14	...	...	0.440	102.6	−17.29
J1016+5823No.3	7.62 ± 0.01(D)	−1.72 ± 0.03	−0.77 ± 0.03	−1.84 ± 0.07	−2.48 ± 0.04	0.020	169.4	−17.29
J1044+0353	7.44 ± 0.01(D)	−1.61 ± 0.03	−0.75 ± 0.02	−1.64 ± 0.04	−2.27 ± 0.04	0.150	257.5	−16.63
J1119+5130	7.51 ± 0.02(D)	−1.64 ± 0.04	−0.78 ± 0.05	−1.69 ± 0.11	−2.60 ± 0.07	0.025	30.4	−14.95
J1132+5722No.1	7.50 ± 0.03(D)	−1.56 ± 0.04	−0.83 ± 0.06	−1.57 ± 0.06	−2.43 ± 0.05	0.140	81.8	−16.48
J1132+5722No.2	7.74 ± 0.03(D)	−1.38 ± 0.04	−0.93 ± 0.07	−1.64 ± 0.08	−2.38 ± 0.05	0.245	41.0	−16.48
J1132+5722No.3	7.68 ± 0.05(D)	−1.44 ± 0.09	−0.86 ± 0.11	...	...	0.235	22.3	−16.48
J1154+4636	7.75 ± 0.02(D)	−1.37 ± 0.03	−0.75 ± 0.04	−1.56 ± 0.05	−2.42 ± 0.04	0.060	89.7	−14.39
J1215+5223	7.53 ± 0.02(D)	−1.56 ± 0.04	−0.80 ± 0.04	−1.63 ± 0.08	−2.38 ± 0.04	0.180	84.1	−12.96
J1224+3724	7.78 ± 0.01(D)	−1.39 ± 0.02	−0.76 ± 0.02	−1.65 ± 0.04	−2.30 ± 0.03	0.145	110.9	−18.83
J1244+3212No.1	7.81 ± 0.03(D)	−1.64 ± 0.02	−0.80 ± 0.03	−1.79 ± 0.03	−2.44 ± 0.02	0.085	78.8	−19.67
J1244+3212No.2	7.90 ± 0.02(D)	−1.66 ± 0.03	−0.81 ± 0.04	−1.71 ± 0.05	−2.44 ± 0.03	0.235	75.2	−19.67
J1244+3212No.3	7.81 ± 0.01(D)	−1.57 ± 0.02	−0.84 ± 0.03	−1.73 ± 0.03	−2.39 ± 0.02	0.090	151.7	−19.67
J1248+4823	7.80 ± 0.01(D)	−1.54 ± 0.03	−0.76 ± 0.02	−1.59 ± 0.03	−2.19 ± 0.03	0.125	114.5	−17.74
J1327+4022	7.70 ± 0.01(D)	−1.37 ± 0.03	−0.77 ± 0.02	−1.37 ± 0.04	−2.07 ± 0.04	0.060	220.9	−14.47
J1331+4151	7.70 ± 0.01(D)	−1.55 ± 0.02	−0.76 ± 0.02	−1.52 ± 0.02	−2.20 ± 0.02	0.135	177.6	−17.07
J1355+4651	7.58 ± 0.01(D)	−1.44 ± 0.07	−0.76 ± 0.02	−1.58 ± 0.07	−2.08 ± 0.06	0.070	353.5	−16.30
J1608+3528	7.79 ± 0.02(D)	−1.70 ± 0.09	−0.68 ± 0.02	...	−2.20 ± 0.09	0.440	367.5	−18.22

Notes. [(a)] Oxygen abundances derived by direct (D) and semi-empirical (E) methods.

Table 9. continued.

Name	12 + log O/H[a]	log N/O	log Ne/O	log S/O	log Ar/O	C (Hβ)	EW (Hβ)	M_g,M_B
c) high-resolution MMT observations								
J0810+1837	7.83 ± 0.20(D)	...	−0.84 ± 0.60	...	...	0.000	8.4	−13.71
J0833+2508No.1	7.69 ± 0.04(D)	...	−0.89 ± 0.10	...	...	0.000	45.4	−14.67
J0833+2508No.2	7.43 ± 0.13(D)	...	−0.78 ± 0.39	...	...	0.095	24.7	−14.67
J0834+5905	7.24 ± 0.08(D)	...	−0.89 ± 0.23	...	...	0.010	28.3	−11.56
J0931+2717No.1	7.45 ± 0.06(E)	...	−1.01 ± 0.22	...	...	0.000	16.5	−14.14
J0931+2717No.2	7.52 ± 0.06(E)	...	−1.01 ± 0.22	...	...	0.000	18.2	−14.14
DDO68 No.3	7.15 ± 0.04(D)	...	−0.81 ± 0.07	...	...	0.000	15.7	−14.54
DDO68 No.4	7.16 ± 0.09(D)	...	−0.92 ± 0.26	...	...	0.000	36.0	−14.54
J0959+4626	7.50 ± 0.05(E)	...	−0.91 ± 0.22	...	...	0.265	57.0	−12.47
J1057+1358No.1	7.18 ± 0.07(E)	...	...	...	...	0.000	8.7	−14.29
J1121+3744No.1	7.12 ± 0.06(E)	...	...	...	...	0.000	8.4	−14.59
J1231+4205	7.62 ± 0.04(D)	...	−0.87 ± 0.10	...	...	0.190	65.7	−12.33

magnitude in the SDSS g band or in the B band whenever available from the literature. Examination of this Table shows that our sample consists of H II regions spanning a wide range of oxygen abundance 12 + log O/H = 7.1–7.9. That range is clearly on the low metallicity side of the roughly Gaussian metallicity distribution of BCDs which peaks at 12 + log O/H ∼ 8.1 (Thuan 2008). For comparison, the 12 + log O/H of the Small and Large Magellanic Clouds and the Sun are respectively 8.03, 8.35 (Russell & Dopita 1992) and 8.69 (Asplund et al. 2009). One of the H II regions, J1121+3744 No.1, has an abnormally low oxygen abundance. We derived 12 + log O/H = 6.78 ± 0.16 from its 3.5 m APO spectrum. However, because of its faintness, the APO spectrum is noisy (Fig. 1), and we have reobserved J1121+3744 No. 1 with the MMT. The oxygen abundance obtained from the MMT spectrum (Fig. 3) is significantly higher, 12+log O/H = 7.12. However, it is still among the lowest known. Note, however, that no [O III] λ4363 emission line is detected, therefore its abundance has been derived using the semi-empirical method, making it less certain. The present sample contains 7 galaxies with 12+log O/H ≤ 7.35. For two galaxies, J0113+0052 and DDO 68, we confirm the very low oxygen abundances first found by Izotov et al. (2006b) and Pustilnik et al. (2005), respectively. As for the remaining five XMD galaxies, J0834+5905, J1056+3608, J1057+1358, J1121+3744 and J1146+4050, their oxygen abundances are derived for the first time in the present paper.

In Table 10 we show, in order of increasing oxygen abundance, the list of the 17 lowest metallicity XMD emission-line galaxies known so far, including the galaxies studied in this paper. It is seen from Table 10 that no H II region with an oxygen abundance 12 + log O/H < 7.1 has been found, except for three H II regions (out of four observed) in SBS 0335–052W. This supports the idea discussed by, e.g., Thuan et al. (2005) that the matter from which dwarf emission-line galaxies formed was pre-enriched to a level 12 + log O/H ≳ 6.9 (or ∼2% of the abundance 12 + log O/H = 8.69 of the Sun, Asplund et al. 2009). Based on *FUSE* spectroscopic data, Thuan et al. (2005) showed that BCDs spanning a wide range in ionised gas metallicities all have H I envelopes with about the same neutral gas metallicity of ∼7.0. This is also the metallicity found in Lyα absorbers (Prochaska et al. 2003). Taken together, the available data suggest that there may have been previous enrichment of the primordial neutral gas to a common metallicity level 12 + log O/H ∼ 6.9, possibly by Population III stars.

As for other heavy elements, we show in Fig. 4 by large circles the location of our sample galaxies in the log N/O, log Ne/O, log S/O and log Ar/O vs. oxygen abundance diagrams. The filled large circles represent galaxies with element abundances determined by the direct method while the open large circles show those with element abundances determined by the semi-empirical method. Examination of Fig. 4 shows that there is no systematic difference between the filled and open large circles. For comparison, smaller filled circles show the galaxies from the sample of Izotov & Thuan (2004a) used for the primordial He abundance determination, and dots show the emission-line galaxies from the SDSS DR3 (Izotov et al. 2006a). In general, the locations of our galaxies are consistent with those obtained for other emission-line galaxies. However, since many of the galaxies studied in this paper are faint and with weak emission lines in their spectra, they show a larger scatter in Fig. 4 as compared to galaxies from the comparison sample. Higher signal-to-noise ratio observations with large telescopes are needed to improve the abundance determination in these galaxies.

Table 10. List of the most metal-deficient emission-line galaxies known.

Name	12 + log O/H[a]	Reference
SBS 0335−052W	6.86–7.22(D)	3
SBS 0335−052E	7.11–7.32(D)	3
J092609.45+334304.1	7.12(D)	10
J1121+3744	7.12(E)	1
DDO68	7.14–7.16(D)	1, 4, 6
J0113+0052	7.15–7.32(D)	1, 2
J1056+3608	7.16–7.32(D)	1
I Zw 18	7.17–7.22(D)	5
J1057+1358	7.18(E)	1
J0834+5905	7.24(D)	1
J2104−0035	7.26(D)	2
J0254+0035	7.28(D)	4
J0812+4836	7.28(D)	4
Leo A	7.30(D)	7
UGCA 292	7.30(D)	8
J1414−0208	7.32(D)	9
J1146+4050	7.34(E)	1

Notes. [(a)] Oxygen abundances derived by direct (D) and semi-empirical (E) methods.

References. (1) this paper; (2) Izotov et al. (2006b); (3) Izotov et al. (2009); (4) Izotov & Thuan (2007); (5) Thuan & Izotov (2005); (6) Izotov & Thuan (2009); (7) Skillman et al. (1989), van Zee et al. (2006); (8) van Zee (2000); (9) Guseva et al. (2007); (10) Pustilnik et al. (2010).

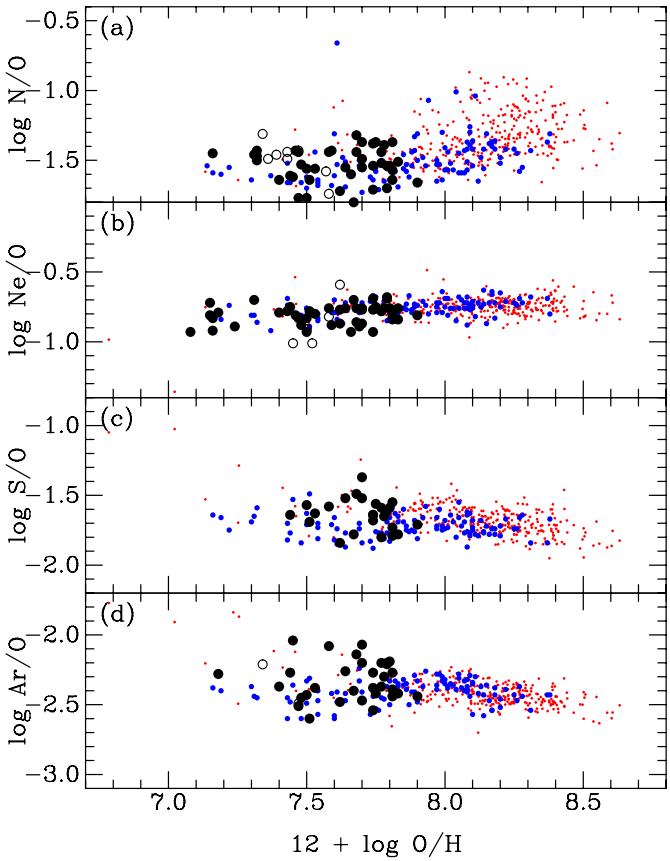

Fig. 4. Abundance ratios vs. oxygen abundance. The emission-line galaxies from this paper are shown by large circles, the filled circles representing galaxies with element abundances derived by the direct method, and the open ones galaxies with element abundances derived by the semi-empirical method; small filled circles are XMD emission-line galaxies from Izotov & Thuan (2004a), and dots are SDSS galaxies from Izotov et al. (2006a).

4. XMD emission-line galaxies and the luminosity–metallicity relation

It was established more than 30 years ago that low-luminosity dwarf galaxies have systematically lower metallicities as compared to more luminous galaxies (Lequeux et al. 1979; Skillman et al. 1989; Richer & McCall 1995). The study of this dependence sheds light on the physics of galaxy and star formation. The relation may also be potentially useful in searching for XMD emission-line galaxies, in addition to our selection criterion based on the fluxes of [O III] λ4959, 5007 and [N II] λ6584 emission lines relative to Hβ.

As a measure of metallicity and luminosity of each galaxy, we adopt respectively the oxygen abundance 12 + log O/H and the absolute magnitude M_g in the g band or M_B in the B band. We will call their dependence on one another the "luminosity−metallicity" or "L−Z" relation. Because Papaderos et al. (2008) have shown that, for emission-line galaxies, the $B-g$ color index is <0.1 mag, we have not transformed B magnitudes to g magnitudes and have used either one, whenever available in the literature. For the galaxy distances, we have selected the ones from the NASA/IPAC Extragalactic Database (NED)[2] which are obtained from the radial velocities corrected for Virgo infall only. Distances and apparent g or B magnitudes are given in Table 1 for all our galaxies. In the cases where several H II regions were observed within the same galaxy, the same distance and g or B magnitude of the whole galaxy were assigned to each H II region. The derived absolute magnitudes M_g or M_B for all the galaxies in our sample are shown in Table 9. They were obtained from the apparent magnitudes in Table 1 and corrected for extinction as defined by C(Hβ) in Table 9 for a single star-forming region, or by the average value of C(Hβ) in the case of multiple knots of star formation.

The luminosity−metallicity diagram for the present sample (Table 1) is shown in Fig. 5a by blue large filled and open circles. The XMD emission-line galaxies discussed by Izotov & Thuan (2007), also selected from the SDSS with the same selection criteria, are shown by red asterisks. For comparison, the dots show the large sample of emission-line galaxies studied by Izotov et al. (2006a). The latter sample includes all emission-line star-forming galaxies from the SDSS DR3 with a reliably detected [O III] λ4363 emission line (its flux is at least 4 times the flux error). The distances to the SDSS DR3 galaxies are derived from their radial velocities, adopting a Hubble constant $H_0 = 75$ km s^{-1} Mpc^{-1}. All nearby objects with $z < 0.003$, and hence with a less certain distance, are excluded from the SDSS DR3 sample. We have also excluded all SDSS galaxies with $z > 0.03$, thus restricting our sample to dwarf galaxies. Totally, the SDSS DR3 sample in Fig. 5a contains 272 galaxies. We have also shown and labelled the most-metal deficient BCDs known, SBS 0335–052W, SBS 0335–052E and I Zw 18, by blue, magenta and red stars, respectively. We show respectively by the solid, dotted, and dot-dashed lines the L–Z relations obtained by Skillman et al. (1989), Richer & McCall (1995), and Berg et al. (2012) for nearby dwarf irregular galaxies.

It can be seen from Fig. 5a that the SDSS DR3 galaxies with $M_g > -18$ mag are slightly offset to brighter magnitudes as compared to the L–Z relations of Skillman et al. (1989), Richer & McCall (1995), and Berg et al. (2012). Fitting the data set composed of the SDSS DR3 galaxies (black dots) and the emission-line galaxies from Izotov & Thuan (2007) (red asterisks) and from the present paper (blue filled and open circles) by a linear regression gives:

$$12 + \log \mathrm{O/H} = -0.108 \times M_g + 6.113. \quad (1)$$

This linear regression is shown in Fig. 5a by a dashed line. It has a slope shallower than the ones of −0.165 from Skillman et al. (1989) and of −0.147 from Richer & McCall (1995). On the other hand, the slope of our relation (Eq. (1)) is the same as that by Berg et al. (2012). However, the relation defined by Eq. (1) is shifted by ~0.2 dex to lower oxygen abundances indicating that we find more metal-poor galaxies with our selection criteria. The spread of the data points about the fit is partially due to observational uncertainties, but also to the way the samples are selected. The SDSS DR3 galaxies have been selected to have a detectable [O III] λ4363 emission line, and hence to have strong star formation, in contrast to the more quiescent dwarf irregular galaxies studied by Skillman et al. (1989) and Richer & McCall (1995). The shallower slope of the relation defined by Eq. (1) as compared to the relations by Skillman et al. (1989) and Richer & McCall (1995) is due to the offset, at a given metallicity, to brighter magnitudes of the SDSS DR3 and emission-line galaxies in the present sample. Guseva et al. (2009) have found that galaxies with such strong ongoing star formation tend to be shifted to brighter magnitudes as compared to galaxies in a more quiescent stage. Using the equivalent

[2] This research has made use of the NASA/IPAC Extragalactic Database (NED) which is operated by the Jet Propulsion Laboratory, California Institute of Technology, under contract with the National Aeronautics and Space Administration.

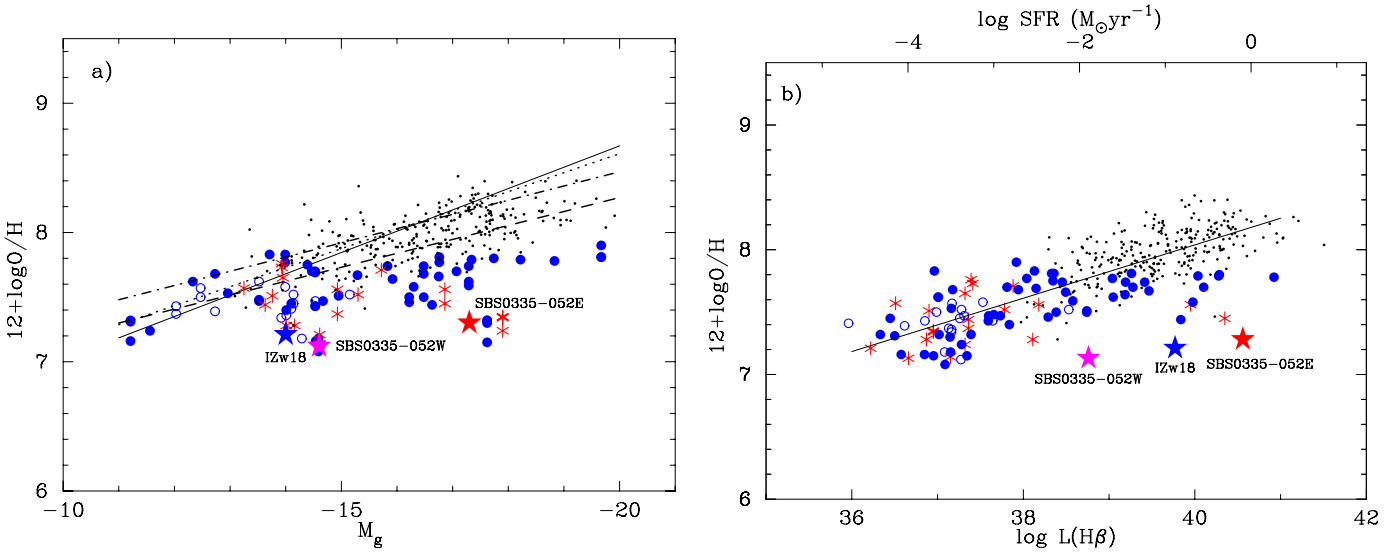

Fig. 5. a) Absolute g magnitude–oxygen abundance relation. The emission-line galaxies from this paper are shown by large circles, the filled circles representing galaxies with element abundances derived by the direct method, and the open ones galaxies with element abundances derived by the semi-empirical method; the XMD emission-line galaxies of Izotov & Thuan (2007) are shown by red asterisks, and the SDSS galaxies of Izotov et al. (2006a) by black dots. The dashed line is the linear regression to all these data. The solid line is the relation derived by Skillman et al. (1989), the dotted line is the one derived by Richer & McCall (1995), and the dot-dashed line is the one derived by Berg et al. (2012). For comparison, the most-metal deficient BCDs I Zw 18, SBS 0335–052W and SBS 0335–052E are shown by blue, magenta and red stars, respectively, and labelled. **b)** Hβ luminosity–oxygen abundance relation. The symbols are the same as in a). The solid line is the linear regression to all data, excluding I Zw 18, SBS 0335–052W and SBS 0335–052E.

width EW(Hβ) of the Hβ emission line as a measure of the relative contribution of star forming regions to the total luminosity of the galaxy, they demonstrated that the galaxies with high EW(Hβ) > 100 Å are brighter in the L–Z diagram as compared to the galaxies with EW(Hβ) < 20 Å.

Thus, the XMD galaxies (asterisks, open and filled circles) do not follow the relations shown by the solid, dashed, and dot-dashed lines. They lie in a horizontal band defined by $7.1 < 12 + \log \mathrm{O/H} < 7.9$, and their metallicities appear to be independent of luminosity over a wide range of galaxy absolute brightnesses $-19 < M_g$, $M_B < -13$. The fact that our emission-line galaxies all have relatively low metallicities is not surprising: it is a result of the way they have been selected, by considering certain emission line flux ratios lying in certain ranges, as described before. What may be more surprising is the very large range of absolute magnitudes $-17 < M_g$, $M_B < -11$ mag for the galaxies with the lowest metallicities ($12 + \log \mathrm{O/H} < 7.5$) in our sample. As examples of extreme outliers, we have indicated by stars the location of three of the most metal-deficient galaxies known, SBS 0335−052W, and SBS 0335−052E and I Zw 18. In particular, for its oxygen abundance, the galaxy SBS 0335−052E is some 5.5 mag brighter than the luminosity expected from the L–Z relation by Skillman et al. (1989) (solid line). This high luminosity is due to the presence of several luminous super-star clusters in SBS 0335−052E (Thuan et al. 1997). Ekta & Chengalur (2010) have attributed the deviations of XMD emission-line galaxies from the L–Z relation to a combination of a high H I gas content (they have processed less gas into stars than other galaxies) and of a more uniform mixing of metals in their ISM due to tidal interactions. Thus, the use of the luminosity−metallicity relation to pick out XMD galaxies, especially the bright ones, is not as reliable as our selection method based on the relative fluxes of emission lines.

In Fig. 5b, we show the relation between the Hβ luminosity L(Hβ) and the oxygen abundance for the same galaxies as in Fig. 5a. The upper abscissa shows the corresponding star formation rate (SFR), derived from the Hα luminosity and the relation $SFR = 7.9 \times 10^{-42} L(\mathrm{H}\alpha)$ of Kennicutt (1998), where SFR is in $M_\odot\,\mathrm{yr}^{-1}$ and L(Hα) is in erg s^{-1}. For $\log L(\mathrm{H}\beta) < 39.5$, it is seen that the emission-line galaxies in both the present and Izotov & Thuan (2007) samples follow nicely the relation defined by the SDSS DR3 galaxies, down to the low-luminosity (or low SFR) range. There appears to be a flattening for $\log L(\mathrm{H}\beta) > 39.5$, but it is a result of our selection criteria which pick out only galaxies with $12 + \log \mathrm{O/H} \lesssim 7.6$–$7.8$. The joint fit to the present, the Izotov & Thuan (2007) and the SDSS DR3 samples gives the linear regression

$$12 + \log \mathrm{O/H} = 0.214 \times \log L(\mathrm{H}\beta) - 0.510, \quad (2)$$

where L(Hβ) is in erg s^{-1}.

From inspection of Fig. 5b, we conclude that the most metal-deficient H II regions, those with $12 + \log \mathrm{O/H} \leq 7.35$, are found among galaxies with the lowest Hβ luminosities, those with $\log L(\mathrm{H}\beta) \lesssim 37.5$. Given that a single O5V star produces a Hβ luminosity of 4.8×10^{36} erg s^{-1} (or $\log L(\mathrm{O5V}) = 36.68$) (Leitherer 1990), this means that only one or a few O stars are sufficient to ionise the ISM in these XMD emission-line galaxies with low L(Hβ). Thus, a good recipe for finding XMD emission-line galaxies would be to search for galaxies with very low Hβ luminosities, those with $\log L(\mathrm{H}\beta) \lesssim 37.5$. However, this is a very challenging task since in these galaxies, the emission lines would be intrinsically weak, and only very nearby XMD emission-line galaxies would be apparently bright enough for reliable abundance determination. There are however a few bright galaxies that are outliers, including three well-known XMD BCDs with $12 + \log \mathrm{O/H} < 7.3$, in Fig. 5b: SBS 0335−052W, SBS 0335−052E and I Zw 18. They are bright because there are presently undergoing an intense starburst with a high SFR. This starburst produces copious amounts of ionising photons resulting in high-excitation H II regions.

In summary, our attempts to find I Zw 18-like or SBS 0335−052-like objects by searching the entire SDSS spectroscopic survey, containing ∼10^6 galaxy spectra, have not been a resounding success. No such galaxy was found in the SDSS, except for I Zw 18 itself. The other two galaxies, SBS 0335−052W and SBS 0335−052E, are outside the sky region covered by the SDSS. Although the number of XMD galaxies with oxygen abundances near the metallicity floor has grown, none of the newly discovered ones listed in Table 10 is both as bright in apparent magnitude and contains high-excitation H II regions as the two well-known prototype XMD BCDs I Zw 18 and SBS 0335–052E, discovered respectively by Sargent & Searle (1970) and Izotov et al. (1990). Because of their brightness and their high-excitation H II regions, these objects have allowed high-sensitivity and high spatial resolution multiwavelength studies of their star formation and chemical evolution properties that none of the newly discovered XMD emission-line galaxies will permit (see Thuan 2008, for a review). After more than 40 years of search for the most metal-poor galaxies, I Zw 18 and SBS 0335–052E still remain the most interesting objects among XMD emission-line galaxies.

5. XMD emission-line galaxies and the emission-line diagnostic diagram

Finally, in Fig. 6 we show the location of the most metal-poor galaxies in the Baldwin-Phillips-Terlevich (BPT) diagnostic diagram (Baldwin et al. 1981) for emission-line galaxies. The cloud of grey dots represents the location of the ∼100 000 SDSS DR7 galaxies. The dashed and solid lines (Kauffmann et al. 2003; Stasińska et al. 2006) separate star-forming galaxies (to the left of the lines) from active galactic nuclei (to the right of the lines). Open black circles are luminous compact galaxies (LCGs) with high SFRs of ∼1−60 $M_\odot$ yr^{-1} which occupy the upper tail of the star-forming galaxy region. LCGs were studied in detail by Izotov et al. (2011) who found that their oxygen abundance distribution peaks at 12 + log O/H of ∼8.0. The emission-line galaxies observed and discussed in the present paper are shown by filled blue circles. They are located below the region where lie the bulk of the star-forming galaxies, a sign of their less advanced chemical evolution and of their lower metallicities. The most metal-deficient galaxies known, listed in Table 10, are shown by red filled circles. We have plotted all observations of these galaxies that we could find in the literature, including multiple observations of SBS 0335–052E. It is evident from Fig. 6 that the lowest-metallicity emission-line galaxies occupy a region of the BPT diagram, which has been left vacant before by the known star-forming galaxy population. The lowest-metallicity galaxies have considerably smaller [O III]/Hβ ratios and generally smaller [N II]/Hα ratios. The Local Group dwarf irregular galaxy Leo A (encircled in Fig. 6) has the highest [O III]/Hβ ratio among the known lowest-metallicity emission-line galaxies. We note that the oxygen abundance for Leo A has been derived from the spectrum of a planetary nebula, not of a H II region (Skillman et al. 1989; van Zee et al. 2006). The fact that this region in the BPT diagram was left empty before suggests that the population of the most metal-poor emission-line galaxies in the local Universe is extremely small. This is born out by our rough search statistics. Out of one million SDSS spectra, we have isolated about 13000 emission-line objects with a detected [O III]λ4363, and out of these there are ∼15 galaxies with 12 + log O/H ≤ 7.35, so the fraction of the most metal-poor emission-line galaxies in the local universe is ∼0.1%.

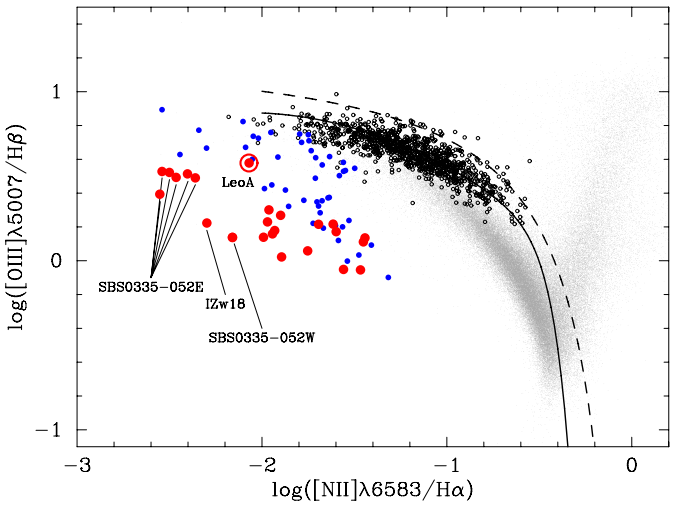

Fig. 6. The Baldwin-Phillips-Terlevich diagram (Baldwin et al. 1981) for emission-line galaxies. The emission-line galaxies observed in this paper are shown by filled blue circles and the most-metal deficient star-forming galaxies known (Table 10) are shown by red filled circles, including observations of several knots of star formation in SBS 0335–052E. The Local Group dwarf irregular galaxy Leo A is encircled. Also, plotted are the 100 000 emission-line galaxies from SDSS DR7 (cloud of grey dots) and a sample of 803 luminous compact galaxies (LCGs, open black circles) (Izotov et al. 2011). The dashed line from Kauffmann et al. (2003) and the solid line from Stasińska et al. (2006) separate star-forming galaxies from active galactic nuclei. The latter lie in the right wing of the "butterfly".

6. Conclusions

We present spectroscopic observations with the 6.5 m MMT and the 3.5 m APO telescope of a sample of 69 H II regions in 42 dwarf emission-line galaxies. These galaxies were selected from the data release 7 (DR7) of the Sloan Digital Sky Survey (SDSS) using mainly two criteria: [O III]λ4959/Hβ ≲ 1 and [N II]λ6583/Hβ ≲ 0.1. These spectral properties select out extremely low-metallicity galaxies, with oxygen abundances comparable to those of the two prototype extremely metal-deficient (XMD) emission-line galaxies SBS 0335–052E and I Zw 18.

Our results are as follows:

1. We find that 14 H II regions in 7 emission-line galaxies have oxygen abundances 12 + log O/H ≤ 7.35. Among them, the 2 galaxies J0113+0052 and DDO 68 have been observed previously. We confirm the very low oxygen abundances for J0113+0052 found by Izotov et al. (2006b) and for DDO 68 found by Pustilnik et al. (2005) and Izotov & Thuan (2007). In addition, we find 5 more galaxies with 12 + log O/H ≤ 7.35. Our data set, when combined with previous studies, results in a total of 17 known XMD emission-line galaxies with 12 + log O/H ≤ 7.35 (Table 10). Among all the emission-line galaxies that have been studied, there is no object that has been discovered with 12 + log O/H < 6.9, although the selection criteria do not forbid such an object. This appears to suggest the existence of an oxygen abundance floor at that level, and supports the idea that the matter from which dwarf emission-line galaxies formed was pre-enriched to a level 12 + log O/H ∼ 6.9 (e.g., Thuan et al. 2005).
2. We have examined the absolute magnitude−metallicity diagram for our emission-line galaxies. We find that these form an horizontal band where the metallicity appears to be nearly independent of luminosity over a wide range (∼8 mag) of

absolute magnitudes, corresponding to a luminosity range of ∼1500. The inclusion of XMD emission-line galaxies in a sample of dwarf star-forming galaxies would make the slope of the absolute magnitude−metallicity relation shallower as compared to samples of more quiescent dwarf irregular galaxies, not including XMD emission-line galaxies, as those of Skillman et al. (1989) and Richer & McCall (1995). On the other hand, we find a tight relation between the Hβ luminosity and the metallicity for the combined sample of XMD and SDSS emission-line galaxies, where the luminosities change by a factor of $\sim 10^5$.

3. Because of the large dispersion about the fit to the absolute magnitude−metallicity relation, the use of the latter is not a good way to select XMD emission-line galaxies. It is more efficient to select them on the basis of flux ratios of nebular [O III] and [N II] relative to Hβ emission lines, and by using the Hβ luminosity−metallicity relation. We find that more than ∼1/3 of the studied H II regions with $\log L(\mathrm{H}\beta) \lesssim 37.5$ are XMD galaxies with $12 + \log \mathrm{O/H} \leq 7.35$. On the other hand, we have failed to find more bright extremely metal-poor emission-line galaxies in the complete SDSS spectroscopic survey, similar to the prototype BCDs SBS 0335−052E and I Zw 18.

Acknowledgements. This research has been supported by NSF grant AST-02-05785 and NASA contract 1263707. Y.I.I. thanks the hospitality of the Astronomy Department of the University of Virginia, USA. Y.I.I. and N.G.G. thank the hospitality of the Max-Planck Institute for Radioastronomy, Bonn, Germany. T.X.T. thanks the hospitality of the Institut d'Astrophysique de Paris. Funding for the Sloan Digital Sky Survey (SDSS) and SDSS-II has been provided by the Alfred P. Sloan Foundation, the Participating Institutions, the National Science Foundation, the US Department of Energy, the National Aeronautics and Space Administration, the Japanese Monbukagakusho, and the Max Planck Society, and the Higher Education Funding Council for England.

References

Aller, L. H. 1984, Physics of Thermal Gaseous Nebulae (Dordrecht: Reidel)
Asplund, M., Grevesse, N., & Sauval, A. J., & Scott, P. 2009, ARA&A, 47, 481
Baldwin, J. A., Phillips, M. M., & Terlevich, R. 1981, PASP, 93, 5
Berg, D. A., Skillman, E. D., Marble, A. R., et al. 2012, ApJ, 754, 98
Brown, W. R., Kewley, L. J., & Geller, M. J. 2008, ApJ, 135, 92
de Vaucouleurs, G., de Vaucouleurs, A., Corwin, H., Jr., et al. 1991, Third Reference Catalogue of Bright Galaxies (New York: Springer)
Doyle, M. T., Drinkwater, M. J., Rohde, D. J., et al. 2005, MNRAS, 361, 34
Ekta, B., & Chengalur, J. N. 2010, MNRAS, 406, 1238
Guseva, N. G., Papaderos, P., Izotov, Y. I., et al. 2003, A&A, 407, 105
Guseva, N. G., Izotov, Y. I., Papaderos, P., & Fricke, K. J. 2007, A&A, 464, 885
Guseva, N. G., Papaderos, P., Meyer, H., Izotov, Y. I., & Fricke, K. J. 2009, A&A, 505, 63
Izotov, Y. I., & Thuan, T. X. 1998a, ApJ, 497, 227
Izotov, Y. I., & Thuan, T. X. 1998b, ApJ, 500, 188
Izotov, Y. I., & Thuan, T. X. 2004a, ApJ, 602, 200
Izotov, Y. I., & Thuan, T. X. 2004b, ApJ, 616, 768
Izotov, Y. I., & Thuan, T. X. 2007, ApJ, 665, 1115
Izotov, Y. I., & Thuan, T. X. 2009, ApJ, 690, 1797
Izotov, Y. I., & Thuan, T. X. 2010, ApJ, 710, L67
Izotov, Y. I., Guseva, N. G., Lipovetsky, V. A., Kniazev, A. Y., & Stepanian, J. A. 1990, Nature, 343, 238
Izotov, Y. I., Thuan, T. X., & Lipovetsky, V. A. 1994, ApJ, 435, 647
Izotov, Y. I., Thuan, T. X., & Lipovetsky, V. A. 1997, ApJS, 108, 1
Izotov, Y. I., Stasińska, G., Guseva, N. G., & Thuan, T. X. 2004, A&A, 632, 210
Izotov, Y. I., Thuan, T. X., & Guseva, N. G. 2005, ApJ, 632, 210
Izotov, Y. I., Stasińska, G., Meynet, G., Guseva, N. G., & Thuan, T. X. 2006a, A&A, 448, 955
Izotov, Y. I., Papaderos, P., Guseva, N. G., Fricke, K. J., & Thuan, T. X. 2006b, A&A, 454, 137
Izotov, Y. I., Thuan, T. X., & Stasińska, G. 2007, ApJ, 662, 15
Izotov, Y. I., Guseva, N. G., Fricke, K. J., & Papaderos, P. 2009, A&A, 503, 61
Izotov, Y. I., Guseva, N. G., & Thuan, T. X. 2011, ApJ, 728, 161
Kakazu, Y., Cowie, L. L., & Hu, E. M. 2007, ApJ, 668, 853
Karachentsev, I. D., Karachentseva, V. E., Huchtmeier, W. K., & Makarov, D. I. 2004, AJ, 127, 2031
Kauffmann, G., Heckman, T. M., Tremonti, C., et al. 2003, MNRAS, 346, 1055
Kennicutt, R. C., Jr. 1998, ARA&A, 36, 189
Kniazev, A. Y., Grebel, E. K., Hao, L., et al. 2003, ApJ, 593, 73
Kniazev, A. Y., Pustilnik, S. A., Grebel, E. K., Lee, H., & Pramskij, A. G. 2004, ApJS, 153, 429
Kunth, D., & Östlin, G. 2000, A&ARv, 10, 1
Leitherer, C. 1990, ApJS, 73, 1
Lequeux, J., Rayo, J. F., Serrano, A., Peimbert, M., & Torres-Peimbert, S. 1979, A&A, 80, 155
Makarova, L., Karachentsev, I. D., Rizzi, L., Tully, R. B., & Korotkova, G. 2009, MNRAS, 397, 1672
Odewahn, S. C., & Aldering, G. 1995, AJ, 110, 2009
Papaderos, P., Guseva, N. G., Izotov, Y. I., & Fricke, K. J. 2008, A&A, 491, 113
Patterson, R. J., & Thuan, T. X. 1996, ApJS, 107, 103
Prochaska, J. X., Gawiser, E., Wolfe, A. M., Castro, S., & Djorgovski, S. G. 2003, ApJ, 595, L9
Pustilnik, S. A., & Martin, J.-M. 2007, A&A, 464, 859
Pustilnik, S. A., Lipovetsky, V. A., Izotov, Y. I., et al. 1997, Astron. Lett., 23, 308
Pustilnik, S. A., Kniazev, A. Y., & Pramskij, A. G. 2005, A&A, 443, 91
Pustilnik, S. A., Teplyakova, A. L., Kniazev, A. Y., Martin, J.-M., & Burenkov, A. N. 2010, MNRAS, 401, 333
Richer, M. G., & McCall, M. L. 1995, ApJ, 445, 642
Russell, S. C., & Dopita. M. A. 1992, ApJ, 384, 508
Sargent, W. L. W., & Searle, L. 1970, ApJ, 162, L155
Skillman, E. D., Kennicutt, R. C., Jr., & Hodge, P. W. 1989, ApJ, 347, 875
Stasińska G. 1990, A&AS, 83, 501
Stasińska, G., & Izotov, Y. I. 2003, A&A, 397, 71
Stasińska, G., Cid Fernandes, R., Mateus, A., Sodré, L., & Asari, N. V. 2006, MNRAS, 371, 972
Steidel, C. C., Adelberger, K. L., Shapley, A. E., et al. 2003, ApJ, 592, 728
Thuan, T. X. 2008, in Low-metallicity Star Formation: From the First Stars to Dwarf Galaxies, eds. L. Hunt, S. C. Madden, & R. Schneider (Cambridge Univ. Press), 348
Thuan, T. X., & Izotov, Y. I. 2005, ApJS, 161, 240
Thuan, T. X., Izotov, Y. I., & Lipovetsky, V. A. 1995, ApJ, 445, 108
Thuan, T. X., Izotov, Y. I., & Lipovetsky, V. A. 1997, ApJ, 477, 661
Thuan, T. X., Lecavelier des Etangs, A., & Izotov, Y. I. 2005, ApJ, 621, 269
van Zee, L. 2000, ApJ, 543, L31
van Zee, L., Skillman, E. D., & Haynes, M. P. 2006, ApJ, 637, 269
Whitford, A. E. 1958, AJ, 63, 201
York, D. G., Adelman, J., Anderson, J. E., Jr., et al. 2000, AJ, 120, 1579

Pages 11 to 36 are available in the electronic edition of the journal at http://www.aanda.org

Table 2. Journal of observations.

Name	Date	Exposure (s)	Position angle (deg)	Airmass	Slit (arcsec)
a) 3.5 m APO observations					
J0113+0052No.1	28 Oct. 2008	2700	+62.8	1.41	1.5
J0113+0052No.2	28 Oct. 2008	2700	+62.8	1.41	1.5
J0113+0052No.3	28 Oct. 2008	2700	+62.8	1.41	1.5
J0113+0052No.4	28 Oct. 2008	2700	+11.9	1.75	1.5
J0138+0020	07 Feb. 2008	1800	+72.3	1.50	1.5
J0834+5905No.1	23 Feb. 2009	1800	+48.0	1.13	2.0
J0834+5905No.2	23 Feb. 2009	1800	+48.0	1.13	2.0
J0843+4025	06 Nov. 2008	2700	+100.8	1.49	1.5
J0851+8416	23 Feb. 2009	1800	+10.0	1.63	2.0
J0906+2528No.1	28 Oct. 2008	3600	−44.6	1.41	1.5
J0906+2528No.2	28 Oct. 2008	3600	−44.6	1.41	1.5
J0908+0517No.1	01 Mar. 2008	1800	−5.7	1.28	1.5
J0908+0517No.2	01 Mar. 2008	1800	−5.7	1.28	1.5
J0950+3127No.1	01 Mar. 2008	1800	+259.2	1.09	1.5
J0950+3127No.2	01 Mar. 2008	1800	+259.2	1.09	1.5
DDO68 No.2	07 Feb. 2008	2700	+111.3	1.70	1.5
DDO68 No.3	07 Feb. 2008	2700	+111.3	1.70	1.5
J1056+3608No.1	01 Mar. 2008	2700	−20.7	1.08	1.5
J1056+3608No.2	01 Mar. 2008	2700	−20.7	1.08	1.5
J1056+3608No.3	01 Mar. 2008	2700	−20.7	1.08	1.5
J1109+2007	23 Feb. 2009	1800	+117.4	1.31	2.0
J1119+0935No.1	01 Mar. 2008	1800	−57.1	1.28	1.5
J1119+0935No.2	01 Mar. 2008	1800	−57.1	1.28	1.5
J1119+0935No.3	01 Mar. 2008	1800	−57.1	1.28	1.5
J1121+3744No.1	01 Mar. 2008	1800	−44.1	1.21	1.5
J1121+3744No.2	01 Mar. 2008	1800	−44.1	1.21	1.5
J1146+4050	01 Mar. 2008	1800	+268.3	1.24	1.5
J1226−0115No.1	26 Apr. 2008	1800	+69.6	1.21	1.5
J1226−0115No.2	26 Apr. 2008	1800	+69.6	1.21	1.5
J1235+2755No.1	13 Apr. 2008	2700	+100.0	1.39	1.5
J1235+2755No.2	13 Apr. 2008	2700	+100.0	1.39	1.5
J1235+2755No.3	13 Apr. 2008	2700	+100.0	1.39	1.5
J1241−0340	26 Apr. 2008	3000	+195.0	1.27	1.5
J1257+3341No.1	01 Mar. 2008	1200	−42.4	1.15	1.5
J1257+3341No.2	01 Mar. 2008	1200	−42.4	1.15	1.5
J1257+3341No.3	01 Mar. 2008	1200	−42.4	1.15	1.5
J1403+5804No.1	01 Mar. 2008	1800	−75.4	1.16	1.5
J1403+5804No.2	01 Mar. 2008	1800	−75.4	1.16	1.5
SBS1420+544	13 Apr. 2008	3300	+118.1	1.50	1.5
PHL293B	15 Nov. 2007	3600	+176.1	1.19	1.5
b) low-resolution MMT observations					
J1016+3754	29 Mar. 2008	1200	+0.0	1.14	1.5
J1016+5823No.1	29 Mar. 2008	1800	+53.0	1.35	1.5
J1016+5823No.2	29 Mar. 2008	1800	+53.0	1.35	1.5
J1016+5823No.3	29 Mar. 2008	1800	+53.0	1.35	1.5
J1044+0353	29 Mar. 2008	1800	+90.0	1.34	1.5
J1119+5130	29 Mar. 2008	1800	+90.0	1.24	1.5
J1132+5722No.1	29 Mar. 2008	2700	−12.0	1.33	1.5
J1132+5722No.2	29 Mar. 2008	2700	−12.0	1.33	1.5
J1132+5722No.3	29 Mar. 2008	2700	−12.0	1.33	1.5
J1154+4636	29 Mar. 2008	1800	+0.0	1.39	1.5
J1215+5223	28 Mar. 2008	2700	+0.0	1.10	1.5
J1224+3724	28 Mar. 2008	1800	+0.0	1.17	1.5
J1244+3212No.1	28 Mar. 2008	1800	+69.0	1.07	1.5
J1244+3212No.2	28 Mar. 2008	1800	+69.0	1.07	1.5
J1244+3212No.3	28 Mar. 2008	1800	+69.0	1.07	1.5
J1248+4823	29 Mar. 2008	2700	+0.0	1.32	1.5
J1327+4022	29 Mar. 2008	1800	+0.0	1.36	1.5
J1331+4151	28 Mar. 2008	1800	+0.0	1.11	1.5
J1355+4651	28 Mar. 2008	2400	+0.0	1.14	1.5
J1608+3528	28 Mar. 2008	2400	+0.0	1.01	1.5

Table 2. continued.

Name	Date	Exposure (s)	Position angle (deg)	Airmass	Slit (arcsec)
c) medium-resolution MMT observations					
J0810+1837	29 Mar. 2008	1800	−69.0	1.03	1.5
J0833+2508No.1	29 Mar. 2008	1800	+0.0	1.02	1.5
J0833+2508No.2	29 Mar. 2008	1800	+0.0	1.02	1.5
J0834+5905	13 Apr. 2010	2700	−78.0	1.16	1.5
J0931+2717No.1	29 Mar. 2008	1800	+25.0	1.01	1.5
J0931+2717No.2	29 Mar. 2008	1800	+25.0	1.01	1.5
DDO68 No.3	28 Mar. 2008	4500	+50.0	1.08	1.5
DDO68 No.4	28 Mar. 2008	4500	+50.0	1.08	1.5
J0959+4626	13 Apr. 2010	2700	+17.0	1.05	1.5
J1057+1358No.1	29 Mar. 2008	1800	+56.0	1.05	1.5
J1057+1358No.2	29 Mar. 2008	1800	+56.0	1.05	1.5
J1121+3744No.1	28 Mar. 2008	1800	−44.0	1.04	1.5
J1121+3744No.2	28 Mar. 2008	1800	−44.0	1.04	1.5
J1231+4205	29 Mar. 2008	1800	+0.0	1.03	1.5

Table 3. Emission line intensities in 3.5 m APO spectra.

Ion	$I(\lambda)/I(\mathrm{H}\beta)$	$I(\lambda)/I(\mathrm{H}\beta)$	$I(\lambda)/I(\mathrm{H}\beta)$	$I(\lambda)/I(\mathrm{H}\beta)$	$I(\lambda)/I(\mathrm{H}\beta)$
			Galaxy		
	J0113+0052No.1	J0113+0052No.2	J0113+0052No.3	J0113+0052No.4	J0138+0020
3727 [O II]	82.51 ± 7.09	198.72 ± 13.11	152.91 ± 10.27	84.76 ± 5.96	224.87 ± 32.55
3868 [Ne III]	23.73 ± 3.41	...	...	...	...
3889 He I + H8	23.86 ± 4.79	...	...	...	...
3968 [Ne III] + H7	20.61 ± 4.08	...	...	...	...
4101 Hδ	26.01 ± 3.87	31.54 ± 3.87	...	...	...
4340 Hγ	49.04 ± 3.41	49.98 ± 5.69	48.05 ± 4.19	46.91 ± 2.77	...
4363 [O III]	7.50 ± 1.50	7.15 ± 2.87	10.35 ± 1.85	1.93 ± 0.75	...
4861 Hβ	100.00 ± 4.18	100.00 ± 5.36	100.00 ± 4.89	100.00 ± 3.19	100.00 ± 13.03
4959 [O III]	60.08 ± 2.72	35.08 ± 2.95	71.36 ± 3.67	65.51 ± 2.25	58.78 ± 8.52
5007 [O III]	188.17 ± 6.04	99.51 ± 4.86	204.93 ± 7.62	188.44 ± 4.81	180.72 ± 17.05
6563 Hα	271.43 ± 8.76	261.22 ± 11.17	268.39 ± 10.16	238.97 ± 6.31	288.26 ± 27.13
6583 [N II]	...	7.55 ± 1.02	...	3.54 ± 0.41	...
6717 [S II]	...	21.57 ± 1.63	15.98 ± 1.15	...	...
6731 [S II]	...	13.03 ± 1.38	7.25 ± 1.00	...	...
$C(\mathrm{H}\beta)$	0.065	0.035	0.115	0.045	0.210
$F(\mathrm{H}\beta)$[a]	6.34	3.22	3.59	7.41	3.80
$EW(\mathrm{H}\beta)$ Å	40.7	20.8	30.0	47.3	20.4
EW(abs) Å	0.10	0.00	1.45	0.95	2.95
	J0834+5905No.1	J0834+5905No.2	J0843+4025	J0851+8416	J0906+2528No.1
3727 [O II]	156.75 ± 10.31	177.28 ± 19.23	260.65 ± 14.55	117.77 ± 4.24	254.94 ± 8.59
3868 [Ne III]	...	...	...	19.09 ± 1.94	17.78 ± 2.60
3889 He I + H8	...	...	...	16.76 ± 2.38	...
3968 [Ne III] + H7	...	...	...	20.83 ± 2.47	...
4101 Hδ	...	...	...	27.40 ± 2.29	...
4340 Hγ	46.64 ± 4.71	47.02 ± 7.41	31.07 ± 3.49	46.85 ± 2.16	46.92 ± 3.19
4363 [O III]	...	...	...	6.14 ± 0.98	4.75 ± 1.61
4861 Hβ	100.00 ± 4.90	100.00 ± 10.42	100.00 ± 4.35	100.00 ± 2.56	100.00 ± 3.31
4959 [O III]	67.32 ± 3.39	49.58 ± 5.88	60.16 ± 2.85	108.01 ± 2.48	55.51 ± 2.02
5007 [O III]	192.48 ± 6.79	146.89 ± 12.16	173.26 ± 5.79	307.38 ± 6.20	166.35 ± 4.37
5876 He I	...	...	...	8.38 ± 0.76	...
6563 Hα	288.43 ± 10.09	288.10 ± 22.98	288.17 ± 9.78	270.57 ± 4.36	276.48 ± 7.27
6583 [N II]	5.94 ± 1.04	...	8.52 ± 1.26	5.25 ± 0.51	5.23 ± 0.65
6717 [S II]	14.57 ± 1.37	33.41 ± 4.24	25.49 ± 1.63	9.59 ± 0.54	23.92 ± 1.01
6731 [S II]	8.62 ± 1.35	19.39 ± 3.23	19.14 ± 1.58	6.05 ± 0.45	19.72 ± 1.06
$C(\mathrm{H}\beta)$	0.285	0.135	0.000	0.135	0.210
$F(\mathrm{H}\beta)$[a]	5.23	2.27	11.92	21.63	7.98
$EW(\mathrm{H}\beta)$ Å	17.9	9.9	16.3	83.6	12.2
EW(abs) Å	0.50	1.35	0.00	0.00	0.50
	J0906+2528No.2	J0908+0517No.1	J0908+0517No.2	J0950+3127No.1	J0950+3127No.2
3727 [O II]	123.03 ± 8.83	229.46 ± 33.20	89.38 ± 2.61	218.80 ± 26.29	201.95 ± 15.29
3835 H9	...	...	5.25 ± 1.08	...	...
3868 [Ne III]	20.75 ± 4.51	...	35.78 ± 1.37	...	...
3889 He I + H8	...	...	19.42 ± 1.24	...	...
3968 [Ne III] + H7	...	...	26.84 ± 1.31	...	...
4101 Hδ	18.24 ± 3.27	...	24.72 ± 1.14	...	...
4340 Hγ	53.99 ± 3.86	46.42 ± 10.57	48.28 ± 1.35	41.93 ± 9.26	50.94 ± 14.33
4363 [O III]	5.55 ± 1.19	...	9.24 ± 0.54	...	6.43 ± 2.79
4471 He I	...	...	3.34 ± 0.41	...	...
4686 He II	...	...	4.01 ± 0.35	...	...
4861 Hβ	100.00 ± 3.83	100.00 ± 10.27	100.00 ± 2.00	100.00 ± 10.31	100.00 ± 8.03
4959 [O III]	77.09 ± 2.87	33.17 ± 5.62	136.64 ± 2.54	42.80 ± 7.04	66.52 ± 3.89
5007 [O III]	222.73 ± 6.48	108.25 ± 9.20	407.46 ± 7.15	123.24 ± 11.23	211.09 ± 8.90
5876 He I	...	...	10.23 ± 0.45	...	...
6300 [O I]	...	...	1.99 ± 0.24	...	...
6312 [S III]	...	...	1.68 ± 0.24	...	...
6563 Hα	278.21 ± 8.29	288.63 ± 21.88	278.00 ± 5.30	287.87 ± 23.97	275.19 ± 12.42
6583 [N II]	5.51 ± 0.59	9.65 ± 2.70	5.42 ± 0.28	...	5.57 ± 1.44
6678 He I	...	...	2.77 ± 0.22	...	4.61 ± 1.59
6717 [S II]	9.23 ± 0.73	29.60 ± 4.02	13.78 ± 0.42	...	18.42 ± 2.00
6731 [S II]	5.15 ± 0.69	21.09 ± 3.56	9.88 ± 0.34	...	11.28 ± 1.64
7065 He I	...	...	2.57 ± 0.20	...	...

Table 3. continued.

Ion	$I(\lambda)/I(H\beta)$	$I(\lambda)/I(H\beta)$	$I(\lambda)/I(H\beta)$	$I(\lambda)/I(H\beta)$	$I(\lambda)/I(H\beta)$
			Galaxy		
7136 [Ar III]	...	...	5.81 ± 0.29	...	7.94 ± 1.69
9069 [S III]	...	10.64 ± 4.02	11.31 ± 0.67	...	...
$C(H\beta)$	0.240	0.410	0.040	0.005	0.140
$F(H\beta)$[a]	6.00	3.22	27.49	1.44	3.23
$EW(H\beta)$ Å	37.1	17.2	197.4	14.5	124.6
EW(abs) Å	0.50	0.35	1.30	0.65	0.40
	DDO68 No.2	DDO68 No.3	J1056+3608No.1	J1056+3608No.2	J1056+3608No.3
3727 [O II]	45.15 ± 2.06	57.83 ± 2.59	69.62 ± 6.07	195.47 ± 10.60	167.46 ± 8.84
3868 [Ne III]	12.07 ± 0.97	6.62 ± 0.89	19.44 ± 3.11	...	27.97 ± 4.62
3889 He I + H8	17.47 ± 1.64	19.81 ± 1.91	20.44 ± 6.59	...	...
3968 [Ne III] + H7	20.75 ± 1.53	21.39 ± 1.78	24.41 ± 4.72	...	...
4101 Hδ	26.31 ± 1.43	28.39 ± 1.67	27.67 ± 3.82	27.85 ± 4.20	27.11 ± 5.30
4340 Hγ	47.39 ± 1.59	46.39 ± 1.70	45.83 ± 2.46	47.82 ± 3.91	44.54 ± 3.70
4363 [O III]	3.50 ± 0.41	2.28 ± 0.53	8.20 ± 1.26	6.73 ± 2.24	5.97 ± 1.51
4471 He I	...	...	4.09 ± 1.31	...	...
4686 He II	6.02 ± 0.39	...	...	...	...
4861 Hβ	100.00 ± 2.10	100.00 ± 2.30	100.00 ± 3.53	100.00 ± 4.45	100.00 ± 4.25
4959 [O III]	45.02 ± 1.05	27.37 ± 0.83	67.83 ± 2.50	47.00 ± 2.72	55.18 ± 2.70
5007 [O III]	139.97 ± 2.69	92.85 ± 2.03	199.88 ± 5.67	136.45 ± 5.18	164.28 ± 5.75
5876 He I	3.01 ± 0.28	6.80 ± 0.50	...	...	...
6563 Hα	262.59 ± 5.14	276.69 ± 5.77	272.90 ± 7.87	238.56 ± 8.68	272.49 ± 9.46
6583 [N II]	...	...	2.98 ± 0.58	8.60 ± 1.12	6.61 ± 1.03
6678 He I	2.61 ± 0.23	2.98 ± 0.25	2.82 ± 0.61	...	...
6717 [S II]	5.83 ± 0.29	4.31 ± 0.30	4.75 ± 0.62	16.72 ± 1.46	13.97 ± 1.21
6731 [S II]	3.28 ± 0.26	3.00 ± 0.27	5.03 ± 0.62	9.39 ± 1.35	8.40 ± 1.00
7065 He I	2.49 ± 0.22	3.17 ± 0.27	...	...	...
7136 [Ar III]	1.85 ± 0.17	...	...	...	...
$C(H\beta)$	0.030	0.005	0.340	0.000	0.000
$F(H\beta)$[a]	32.35	29.50	4.56	3.05	4.48
$EW(H\beta)$ Å	191.6	85.3	134.4	31.7	32.5
EW(abs) Å	0.95	1.55	5.60	0.00	1.50
	J1109+2007	J1119+0935No.1	J1119+0935No.2	J1119+0935No.3	J1121+3744No.1
3727 [O II]	275.83 ± 11.86	151.10 ± 7.89	156.59 ± 4.31	286.91 ± 35.82	35.74 ± 22.87
3868 [Ne III]	...	...	17.91 ± 1.45	...	...
3889 He I + H8	...	...	18.35 ± 1.71	...	...
3968 [Ne III] + H7	...	...	15.58 ± 1.61	...	...
4101 Hδ	...	...	25.05 ± 1.51	...	...
4340 Hγ	49.93 ± 3.46	46.75 ± 3.80	49.10 ± 1.70	46.64 ± 9.23	...
4363 [O III]	10.22 ± 2.11	...	3.89 ± 0.59	...	...
4861 Hβ	100.00 ± 3.65	100.00 ± 3.90	100.00 ± 2.24	100.00 ± 10.10	100.00 ± 28.73
4959 [O III]	69.97 ± 2.64	73.12 ± 2.91	78.35 ± 1.73	19.19 ± 4.59	20.65 ± 10.06
5007 [O III]	226.23 ± 6.35	223.44 ± 6.69	236.37 ± 4.54	79.81 ± 8.12	59.47 ± 15.83
5876 He I	...	...	7.68 ± 0.45	...	...
6563 Hα	271.38 ± 7.84	288.01 ± 8.88	281.93 ± 5.70	146.79 ± 12.40	287.90 ± 52.54
6583 [N II]	5.73 ± 0.84	6.65 ± 0.87	7.04 ± 0.34	13.44 ± 2.39	...
6678 He I	...	4.25 ± 0.89	2.50 ± 0.28	...	...
6717 [S II]	22.29 ± 1.23	20.63 ± 1.29	17.08 ± 0.53	...	...
6731 [S II]	15.43 ± 1.17	14.81 ± 1.29	11.97 ± 0.44	...	...
7065 He I	...	1.19 ± 0.57	1.60 ± 0.21	...	...
7136 [Ar III]	...	2.58 ± 0.64	3.47 ± 0.28	...	...
9069 [S III]	...	10.60 ± 2.31	10.96 ± 0.63	...	...
$C(H\beta)$	0.350	0.055	0.225	0.280	0.000
$F(H\beta)$[a]	9.04	10.25	21.94	2.13	0.94
$EW(H\beta)$ Å	22.6	18.7	57.6	29.5	8.9
EW(abs) Å	0.00	1.05	0.45	1.15	3.10
	J1146+4050	J1226-0115No.1	J1226-0115No.2	J1235+2755No.1	J1235+2755No.2
3727 [O II]	191.22 ± 13.38	94.02 ± 1.91	86.25 ± 1.77	208.43 ± 7.19	188.91 ± 3.61
3798 H10	...	5.65 ± 0.88	4.00 ± 0.72	...	4.27 ± 0.80
3835 H9	...	6.64 ± 0.85	5.93 ± 0.72	...	6.59 ± 0.83
3868 [Ne III]	...	44.14 ± 1.01	35.23 ± 0.86	23.36 ± 2.49	32.24 ± 0.95
3889 He I + H8	...	17.86 ± 0.83	19.75 ± 0.76	28.04 ± 3.84	20.37 ± 0.98
3968 [Ne III] + H7	...	29.02 ± 0.89	25.40 ± 0.78	27.24 ± 3.56	24.47 ± 0.92

Table 3. continued.

Ion	$I(\lambda)/I(\mathrm{H}\beta)$	$I(\lambda)/I(\mathrm{H}\beta)$	$I(\lambda)/I(\mathrm{H}\beta)$	$I(\lambda)/I(\mathrm{H}\beta)$	$I(\lambda)/I(\mathrm{H}\beta)$
			Galaxy		
4101 Hδ	...	24.57 ± 0.79	24.70 ± 0.70	24.60 ± 2.52	25.43 ± 0.83
4340 Hγ	49.58 ± 5.61	48.06 ± 0.95	48.44 ± 0.92	49.30 ± 2.41	48.86 ± 1.00
4363 [O III]	...	12.74 ± 0.40	10.03 ± 0.33	9.49 ± 1.50	5.67 ± 0.33
4471 He I	...	3.78 ± 0.25	3.73 ± 0.21	...	3.18 ± 0.24
4686 He II	...	...	1.33 ± 0.17	...	...
4711 [Ar IV] + He I	...	2.03 ± 0.19	1.79 ± 0.19	...	...
4740 [Ar IV]	...	0.98 ± 0.15	0.93 ± 0.18	...	...
4861 Hβ	100.00 ± 5.92	100.00 ± 1.61	100.00 ± 1.57	100.00 ± 2.93	100.00 ± 1.66
4959 [O III]	36.42 ± 3.01	184.60 ± 2.84	168.09 ± 2.55	75.53 ± 2.20	114.40 ± 1.85
5007 [O III]	123.56 ± 6.19	559.52 ± 8.48	513.06 ± 7.69	227.67 ± 5.46	341.13 ± 5.32
5876 He I	...	11.66 ± 0.26	11.15 ± 0.25	8.45 ± 0.76	10.10 ± 0.30
6300 [O I]	...	2.77 ± 0.11	2.04 ± 0.10	...	3.11 ± 0.17
6312 [S III]	...	1.55 ± 0.09	1.70 ± 0.10	...	1.25 ± 0.15
6363 [O I]	...	1.09 ± 0.09	...	...	0.69 ± 0.13
6563 Hα	288.24 ± 12.94	278.39 ± 4.57	280.60 ± 4.56	271.05 ± 6.82	281.10 ± 4.73
6583 [N II]	11.22 ± 1.68	4.45 ± 0.12	5.04 ± 0.13	4.56 ± 0.44	7.96 ± 0.21
6678 He I	...	3.16 ± 0.11	2.95 ± 0.10	...	2.89 ± 0.13
6717 [S II]	21.27 ± 1.87	10.31 ± 0.21	9.64 ± 0.19	13.05 ± 0.60	13.31 ± 0.29
6731 [S II]	13.49 ± 1.68	6.82 ± 0.16	7.37 ± 0.16	9.21 ± 0.56	9.09 ± 0.22
7065 He I	...	3.90 ± 0.12	2.35 ± 0.09	...	2.15 ± 0.12
7136 [Ar III]	3.98 ± 1.49	6.17 ± 0.16	5.30 ± 0.13	...	5.15 ± 0.17
9069 [S III]	...	9.11 ± 0.28	9.34 ± 0.26	7.73 ± 0.84	12.49 ± 0.40
$C(\mathrm{H}\beta)$	0.110	0.130	0.275	0.105	0.075
$F(\mathrm{H}\beta)$[a]	3.72	71.45	85.39	16.35	69.90
$EW(\mathrm{H}\beta)$ Å	17.9	158.5	149.2	36.7	129.8
EW(abs) Å	0.15	1.55	0.90	1.40	0.30
	J1235+2755No.3	J1241-0340	J1257+3341No.1	J1257+3341No.2	J1257+3341No.3
3727 [O II]	234.09 ± 4.97	127.94 ± 2.28	151.42 ± 6.06	302.45 ± 19.12	199.58 ± 6.52
3798 H10	...	4.32 ± 0.59	...	...	...
3835 H9	7.94 ± 1.21	6.24 ± 0.59	...	...	8.13 ± 2.32
3868 [Ne III]	34.45 ± 1.38	51.69 ± 1.02	16.05 ± 1.57	39.59 ± 6.07	16.70 ± 2.10
3889 He I + H8	21.41 ± 1.31	21.74 ± 0.69	16.23 ± 2.60	...	15.94 ± 2.57
3968 [Ne III] + H7	26.17 ± 1.37	29.30 ± 0.72	18.12 ± 2.85	...	19.46 ± 2.21
4101 Hδ	29.29 ± 1.13	27.82 ± 0.64	27.96 ± 2.51	32.48 ± 7.31	22.74 ± 2.04
4340 Hγ	53.74 ± 1.30	48.89 ± 0.87	48.77 ± 2.59	54.78 ± 6.58	49.47 ± 2.17
4363 [O III]	7.23 ± 0.53	11.96 ± 0.32	3.46 ± 0.99	...	3.98 ± 0.94
4471 He I	3.10 ± 0.35	4.09 ± 0.26	...	...	...
4711 [Ar IV] + He I	...	1.35 ± 0.12	...	...	...
4861 Hβ	100.00 ± 1.85	100.00 ± 1.53	100.00 ± 3.11	100.00 ± 6.15	100.00 ± 2.68
4959 [O III]	115.45 ± 2.03	168.08 ± 2.52	49.22 ± 1.73	57.96 ± 4.22	51.88 ± 1.62
5007 [O III]	352.16 ± 5.85	502.34 ± 7.44	161.46 ± 4.25	163.64 ± 8.05	158.82 ± 3.79
5876 He I	11.65 ± 0.39	10.41 ± 0.22	...	...	6.09 ± 0.58
6300 [O I]	2.79 ± 0.20	2.75 ± 0.11	...	...	...
6312 [S III]	1.41 ± 0.15	1.69 ± 0.11	...	...	...
6363 [O I]	0.83 ± 0.01	1.09 ± 0.12	...	...	...
6563 Hα	279.89 ± 5.00	278.97 ± 4.47	278.44 ± 7.22	276.43 ± 7.53	279.53 ± 4.42
6583 [N II]	8.89 ± 0.26	4.58 ± 0.11	6.94 ± 0.65	...	7.62 ± 0.49
6678 He I	2.84 ± 0.19	2.98 ± 0.10	3.65 ± 0.59	...	...
6717 [S II]	14.01 ± 0.35	10.21 ± 0.19	13.01 ± 0.80	...	9.68 ± 0.61
6731 [S II]	9.60 ± 0.28	7.30 ± 0.16	9.83 ± 0.76	...	8.34 ± 0.64
7065 He I	3.00 ± 0.17	2.54 ± 0.08	1.86 ± 0.39	...	...
7136 [Ar III]	5.91 ± 0.21	5.97 ± 0.13	2.16 ± 0.45	...	2.80 ± 0.53
9069 [S III]	13.75 ± 0.48	10.19 ± 0.27	...	...	10.30 ± 1.15
$C(\mathrm{H}\beta)$	0.220	0.310	0.055	0.000	0.000
$F(\mathrm{H}\beta)$[a]	40.80	66.07	12.71	3.71	16.61
$EW(\mathrm{H}\beta)$ Å	156.6	125.3	75.7	22.8	90.6
EW(abs) Å	0.25	0.25	0.00	0.00	0.00
	J1403+5804No.1	J1403+5804No.2	SBS 1420+544	PHL293B	
3727 [O II]	159.09 ± 13.42	120.35 ± 4.53	57.64 ± 1.58	108.65 ± 2.41	
3750 H12	...	...	4.34 ± 1.36	...	
3771 H11	...	...	3.65 ± 1.16	...	
3798 H10	...	...	6.64 ± 1.08	...	
3835 H9	...	...	11.12 ± 1.04	6.14 ± 1.13	

Table 3. continued.

Ion	$I(\lambda)/I(\mathrm{H}\beta)$	$I(\lambda)/I(\mathrm{H}\beta)$	$I(\lambda)/I(\mathrm{H}\beta)$	$I(\lambda)/I(\mathrm{H}\beta)$	$I(\lambda)/I(\mathrm{H}\beta)$
			Galaxy		
3868 [Ne III]	...	27.73 ± 2.19	60.40 ± 1.31	47.50 ± 1.19	
3889 He I + H8	...	22.39 ± 2.68	21.21 ± 1.00	18.95 ± 1.11	
3968 [Ne III] + H7	...	22.87 ± 2.70	32.85 ± 1.06	28.59 ± 1.08	
4026 He I	...	...	2.06 ± 0.37	...	
4101 Hδ	...	29.69 ± 2.21	28.13 ± 0.92	29.53 ± 1.03	
4340 Hγ	44.01 ± 7.00	51.24 ± 2.39	46.21 ± 1.04	47.26 ± 1.06	
4363 [O III]	...	9.31 ± 1.04	15.84 ± 0.46	11.93 ± 0.40	
4471 He I	...	...	3.99 ± 0.34	3.89 ± 0.27	
4658 C III/C IV	...	...	...	1.00 ± 0.15	
4658 [Fe III]	...	...	...	1.00 ± 0.15	
4686 He II	...	...	...	0.88 ± 0.14	
4711 [Ar IV] + He I	...	...	3.13 ± 0.27	2.04 ± 0.20	
4740 [Ar IV]	...	...	1.67 ± 0.24	1.07 ± 0.18	
4861 Hβ	100.00 ± 6.50	100.00 ± 2.56	100.00 ± 1.70	100.00 ± 1.66	
4921 He I	...	...	...	2.04 ± 0.18	
4959 [O III]	51.54 ± 4.21	94.56 ± 2.17	216.13 ± 3.41	158.18 ± 2.45	
5007 [O III]	156.08 ± 7.95	281.43 ± 5.68	665.97 ± 10.36	463.49 ± 7.05	
5876 He I	...	...	10.25 ± 0.24	10.17 ± 0.31	
6300 [O I]	...	...	1.37 ± 0.12	1.63 ± 0.14	
6312 [S III]	...	...	1.18 ± 0.13	1.06 ± 0.14	
6563 Hα	288.00 ± 14.22	274.79 ± 5.91	277.75 ± 4.70	277.23 ± 4.58	
6583 [N II]	6.19 ± 1.59	3.11 ± 0.44	2.19 ± 0.13	2.12 ± 0.11	
6678 He I	...	2.13 ± 0.35	2.55 ± 0.13	2.79 ± 0.16	
6717 [S II]	12.55 ± 2.26	8.45 ± 0.51	5.29 ± 0.15	7.25 ± 0.20	
6731 [S II]	10.75 ± 2.07	6.09 ± 0.49	3.66 ± 0.17	4.78 ± 0.17	
7065 He I	...	1.85 ± 0.37	3.89 ± 0.13	1.97 ± 0.11	
7136 [Ar III]	...	3.43 ± 0.47	4.38 ± 0.15	3.87 ± 0.13	
9069 [S III]	...	8.34 ± 0.82	10.20 ± 0.39	5.63 ± 0.25	
$C(\mathrm{H}\beta)$	0.070	0.180	0.105	0.115	
$F(\mathrm{H}\beta)$[a]	5.09	18.65	90.23	314.30	
$EW(\mathrm{H}\beta)$ Å	9.1	46.4	201.8	69.6	
EW(abs) Å	0.80	0.15	1.55	0.10	

[a] In 10^{-16} erg s^{-1} cm^{-2}.

Table 4. Emission line intensities in low-resolution MMT spectra.

Ion	$I(\lambda)/I(\mathrm{H}\beta)$	$I(\lambda)/I(\mathrm{H}\beta)$	$I(\lambda)/I(\mathrm{H}\beta)$	$I(\lambda)/I(\mathrm{H}\beta)$	$I(\lambda)/I(\mathrm{H}\beta)$
			Galaxy		
	J1016+3754	J1016+5823No.1	J1016+5823No.2	J1016+5823No.3	J1044+0353
3727 [O II]	62.50 ± 1.26	114.63 ± 2.03	134.53 ± 5.63	104.00 ± 2.04	32.64 ± 0.70
3750 H12	3.14 ± 0.76	2.61 ± 0.63	...	3.00 ± 0.83	3.07 ± 0.37
3771 H11	3.81 ± 0.82	2.93 ± 0.58	...	3.30 ± 0.79	3.95 ± 0.38
3798 H10	4.19 ± 0.67	4.07 ± 0.52	...	4.44 ± 0.76	5.38 ± 0.36
3820 He I	...	1.09 ± 0.35	...	...	...
3835 H9	6.35 ± 0.59	5.83 ± 0.52	...	6.17 ± 0.76	7.12 ± 0.36
3868 [Ne III]	39.33 ± 0.70	34.98 ± 0.67	17.61 ± 1.67	34.66 ± 0.77	36.66 ± 0.63
3889 He I + H8	19.06 ± 0.61	18.79 ± 0.59	22.58 ± 3.30	19.87 ± 0.82	19.98 ± 0.46
3968 [Ne III] + H7	26.04 ± 0.64	25.39 ± 0.62	19.69 ± 2.12	26.44 ± 0.79	26.85 ± 0.52
4026 He I	1.50 ± 0.18	1.45 ± 0.20	...	1.42 ± 0.22	1.76 ± 0.08
4068 [S II]	...	1.62 ± 0.18	...	...	0.46 ± 0.10
4101 Hδ	25.47 ± 0.58	24.81 ± 0.59	27.65 ± 1.94	27.27 ± 0.76	26.53 ± 0.49
4340 Hγ	47.84 ± 0.80	48.07 ± 0.83	41.82 ± 1.67	49.45 ± 0.93	47.39 ± 0.75
4363 [O III]	12.01 ± 0.25	8.42 ± 0.22	4.70 ± 0.73	9.99 ± 0.28	14.25 ± 0.26
4387 He I	...	...	...	...	0.27 ± 0.07
4471 He I	3.43 ± 0.16	3.46 ± 0.17	...	3.52 ± 0.23	3.71 ± 0.13
4658 [Fe III]	1.10 ± 0.15	0.73 ± 0.14	...	0.97 ± 0.19	...
4686 He II	3.02 ± 0.18	1.19 ± 0.16	...	0.77 ± 0.16	2.05 ± 0.10
4711 [Ar IV] + He I	2.07 ± 0.18	0.89 ± 0.13	...	1.28 ± 0.18	2.09 ± 0.10
4740 [Ar IV]	1.36 ± 0.15	...	...	...	1.08 ± 0.08
4861 Hβ	100.00 ± 1.49	100.00 ± 1.52	100.00 ± 2.43	100.00 ± 1.56	100.00 ± 1.47
4921 He I	0.88 ± 0.10	0.79 ± 0.11	...	1.27 ± 0.16	1.00 ± 0.08
4959 [O III]	157.15 ± 2.30	138.19 ± 2.05	80.35 ± 1.89	135.33 ± 2.04	144.12 ± 2.10
4988 [Fe III]	...	0.85 ± 0.08	...	1.33 ± 0.13	...
5007 [O III]	468.92 ± 6.83	409.76 ± 6.01	235.76 ± 4.86	397.74 ± 5.91	426.01 ± 6.17
5199 [N I]	0.34 ± 0.07	0.71 ± 0.10	...	...	...
5876 He I	9.73 ± 0.22	9.18 ± 0.22	9.37 ± 0.57	8.73 ± 0.25	9.64 ± 0.18
6300 [O I]	1.36 ± 0.11	2.32 ± 0.13	...	1.79 ± 0.19	1.05 ± 0.08
6312 [S III]	1.52 ± 0.11	1.40 ± 0.12	...	0.79 ± 0.15	0.79 ± 0.08
6363 [O I]	0.62 ± 0.11	0.84 ± 0.11	...	0.69 ± 0.17	0.34 ± 0.08
6563 Hα	277.14 ± 4.39	240.33 ± 3.85	281.44 ± 6.24	276.87 ± 4.48	274.27 ± 4.33
6583 [N II]	2.26 ± 0.14	2.93 ± 0.15	6.41 ± 0.44	2.45 ± 0.18	0.99 ± 0.08
6678 He I	2.59 ± 0.14	2.68 ± 0.17	...	2.55 ± 0.20	2.70 ± 0.11
6717 [S II]	4.77 ± 0.16	8.84 ± 0.22	18.07 ± 0.75	8.26 ± 0.27	2.61 ± 0.10
6731 [S II]	3.61 ± 0.15	5.96 ± 0.19	11.79 ± 0.65	4.96 ± 0.22	2.03 ± 0.07
7065 He I	2.52 ± 0.16	1.50 ± 0.14	...	1.80 ± 0.26	3.04 ± 0.12
7136 [Ar III]	3.83 ± 0.18	3.13 ± 0.18	...	2.98 ± 0.26	2.28 ± 0.11
7320 [O II]	...	...	...	...	0.56 ± 0.06
7330 [O II]	...	...	...	...	0.57 ± 0.07
$C(\mathrm{H}\beta)$	0.115	0.000	0.440	0.020	0.150
$F(\mathrm{H}\beta)^{ma}$	248.60	103.70	9.15	71.09	136.70
$EW(\mathrm{H}\beta)$ Å	96.3	125.8	102.6	169.4	257.5
EW(abs) Å	0.80	0.35	5.85	0.15	0.30
	J1119+5130	J1132+5722No.1	J1132+5722No.2	J1132+5722No.3	J1154+4636
3727 [O II]	101.26 ± 2.34	110.67 ± 2.37	139.99 ± 4.00	144.75 ± 7.42	137.76 ± 3.12
3835 H9	...	...	...	...	8.37 ± 1.31
3868 [Ne III]	25.33 ± 0.88	17.80 ± 0.62	20.46 ± 1.12	30.55 ± 2.71	35.63 ± 0.97
3889 He I + H8	21.32 ± 1.94	18.55 ± 0.85	20.98 ± 2.04	14.21 ± 4.08	20.95 ± 1.07
3968 [Ne III] + H7	23.13 ± 1.45	18.89 ± 0.81	20.72 ± 2.17	12.98 ± 3.19	23.58 ± 1.02
4101 Hδ	27.30 ± 1.22	25.38 ± 0.72	26.45 ± 1.52	24.57 ± 2.75	26.78 ± 0.87
4340 Hγ	48.39 ± 1.06	47.67 ± 0.90	46.32 ± 1.31	47.23 ± 2.39	46.73 ± 1.01
4363 [O III]	6.75 ± 0.35	4.55 ± 0.30	6.23 ± 0.47	10.06 ± 1.23	7.68 ± 0.39
4471 He I	1.50 ± 0.30	3.29 ± 0.25	1.64 ± 0.39	...	3.30 ± 0.31
4658 [Fe III]	...	...	...	...	1.56 ± 0.25
4686 He II	1.76 ± 0.25	1.52 ± 0.23	...	...	2.52 ± 0.28
4861 Hβ	100.00 ± 1.73	100.00 ± 1.61	100.00 ± 1.95	100.00 ± 2.86	100.00 ± 1.67
4921 He I	...	...	...	...	1.02 ± 0.19
4959 [O III]	91.24 ± 1.56	69.79 ± 1.13	111.83 ± 2.08	138.02 ± 3.39	128.58 ± 2.06
4988 [Fe III]	1.05 ± 0.20	1.41 ± 0.15	...	...	2.34 ± 0.30
5007 [O III]	267.33 ± 4.39	209.51 ± 3.26	337.53 ± 5.98	414.01 ± 9.18	382.09 ± 5.95
5876 He I	9.96 ± 0.34	10.05 ± 0.29	9.40 ± 0.50	12.42 ± 1.16	9.52 ± 0.39
6300 [O I]	1.37 ± 0.26	4.24 ± 0.22	3.14 ± 0.37	...	2.63 ± 0.26

Table 4. continued.

Ion	$I(\lambda)/I(\mathrm{H}\beta)$	$I(\lambda)/I(\mathrm{H}\beta)$	$I(\lambda)/I(\mathrm{H}\beta)$	$I(\lambda)/I(\mathrm{H}\beta)$	$I(\lambda)/I(\mathrm{H}\beta)$
			Galaxy		
6312 [S III]	1.02 ± 0.32	1.10 ± 0.17	1.38 ± 0.29	...	1.91 ± 0.24
6363 [O I]	1.12 ± 0.02	1.30 ± 0.19	...	...	0.97 ± 0.23
6563 Hα	276.84 ± 4.94	279.00 ± 4.70	281.00 ± 5.45	278.34 ± 6.92	279.28 ± 4.76
6583 [N II]	2.86 ± 0.27	3.89 ± 0.26	7.75 ± 0.46	6.46 ± 1.15	7.69 ± 0.38
6678 He I	2.25 ± 0.28	2.85 ± 0.23	2.94 ± 0.40	5.74 ± 1.27	2.72 ± 0.34
6717 [S II]	7.30 ± 0.37	12.89 ± 0.34	16.95 ± 0.60	15.87 ± 1.20	16.71 ± 0.50
6731 [S II]	5.84 ± 0.35	10.31 ± 0.30	11.65 ± 0.53	9.79 ± 1.19	12.89 ± 0.49
7065 He I	2.60 ± 0.22	2.39 ± 0.25	1.40 ± 0.45	...	1.71 ± 0.34
7136 [Ar III]	1.91 ± 0.27	2.65 ± 0.28	4.71 ± 0.44	...	4.44 ± 0.36
7320 [O II]	...	1.44 ± 0.18	2.53 ± 0.45	...	...
7330 [O II]	...	0.84 ± 0.15	2.28 ± 0.44	...	...
$C(\mathrm{H}\beta)$	0.025	0.140	0.245	0.235	0.060
$F(\mathrm{H}\beta)$[a]	81.29	47.54	19.41	6.11	43.26
$EW(\mathrm{H}\beta)$ Å	30.4	81.8	41.0	22.3	89.7
EW(abs) Å	2.85	2.85	4.50	0.85	1.80
	J1215+5223	J1224+3724	J1244+3212No.1	J1244+3212No.2	J1244+3212No.3
3727 [O II]	109.96 ± 2.43	94.09 ± 1.60	196.21 ± 3.20	168.02 ± 3.46	200.05 ± 3.26
3750 H12	...	4.90 ± 0.85	1.91 ± 0.56	...	3.22 ± 0.62
3771 H11	...	5.45 ± 0.67	2.78 ± 0.53	...	4.05 ± 0.56
3798 H10	...	6.55 ± 0.59	2.79 ± 0.48	...	4.28 ± 0.53
3835 H9	6.04 ± 0.94	8.13 ± 0.46	4.56 ± 0.49	7.42 ± 1.65	6.61 ± 0.45
3868 [Ne III]	22.67 ± 0.66	46.94 ± 0.82	32.51 ± 0.60	34.47 ± 0.91	25.86 ± 0.49
3889 He I + H8	19.04 ± 0.83	20.09 ± 0.51	17.56 ± 0.56	17.76 ± 0.98	18.78 ± 0.52
3968 [Ne III] + H7	20.30 ± 0.74	31.81 ± 0.63	23.52 ± 0.58	25.61 ± 0.96	23.90 ± 0.53
4026 He I	...	1.13 ± 0.16	0.75 ± 0.16	...	1.20 ± 0.14
4068 [S II]	...	1.06 ± 0.16	1.54 ± 0.14	...	1.87 ± 0.15
4101 Hδ	25.76 ± 0.73	26.27 ± 0.54	25.19 ± 0.56	25.20 ± 0.85	26.36 ± 0.52
4340 Hγ	47.78 ± 0.90	47.12 ± 0.78	47.77 ± 0.79	47.19 ± 0.97	47.15 ± 0.76
4363 [O III]	6.01 ± 0.29	12.90 ± 0.28	6.84 ± 0.19	7.39 ± 0.36	5.47 ± 0.15
4471 He I	3.42 ± 0.27	3.20 ± 0.17	3.35 ± 0.16	3.33 ± 0.34	3.25 ± 0.12
4658 [Fe III]	...	0.90 ± 0.11	0.58 ± 0.15	...	0.69 ± 0.09
4686 He II	...	1.03 ± 0.09	0.84 ± 0.15	...	...
4711 [Ar IV] + He I	...	1.35 ± 0.11	0.45 ± 0.10	...	...
4740 [Ar IV]	...	1.25 ± 0.11	...	...	...
4861 Hβ	100.00 ± 1.57	100.00 ± 1.52	100.00 ± 1.48	100.00 ± 1.63	100.00 ± 1.47
4921 He I	...	0.88 ± 0.11	0.83 ± 0.15	...	0.87 ± 0.08
4959 [O III]	87.91 ± 1.37	189.11 ± 2.83	122.44 ± 1.78	148.86 ± 2.35	106.52 ± 1.55
4988 [Fe III]	...	1.31 ± 0.11	...	...	...
5007 [O III]	262.56 ± 3.96	557.71 ± 8.29	368.83 ± 5.32	447.94 ± 6.92	318.37 ± 4.61
5199 [N I]	...	...	...	...	0.59 ± 0.08
5518 [Cl III]	...	0.60 ± 0.01	...	...	...
5538 [Cl III]	...	0.27 ± 0.00	...	...	...
5876 He I	10.35 ± 0.30	10.88 ± 0.25	9.68 ± 0.21	9.18 ± 0.28	9.90 ± 0.20
6300 [O I]	...	2.02 ± 0.13	3.11 ± 0.13	2.26 ± 0.20	2.77 ± 0.11
6312 [S III]	1.27 ± 0.23	1.38 ± 0.12	1.27 ± 0.10	1.65 ± 0.19	1.41 ± 0.10
6363 [O I]	...	0.45 ± 0.10	0.98 ± 0.11	...	0.95 ± 0.10
6563 Hα	278.62 ± 4.57	278.38 ± 4.52	280.15 ± 4.39	281.96 ± 4.76	280.92 ± 4.42
6583 [N II]	3.73 ± 0.25	4.96 ± 0.19	5.94 ± 0.16	5.20 ± 0.23	7.36 ± 0.17
6678 He I	2.91 ± 0.24	2.96 ± 0.17	2.81 ± 0.15	2.69 ± 0.22	2.78 ± 0.13
6717 [S II]	6.01 ± 0.25	8.51 ± 0.22	13.84 ± 0.27	11.98 ± 0.34	14.75 ± 0.27
6731 [S II]	4.20 ± 0.24	6.04 ± 0.19	10.10 ± 0.22	9.13 ± 0.30	10.31 ± 0.21
7065 He I	2.32 ± 0.30	2.91 ± 0.17	1.60 ± 0.15	2.69 ± 0.25	1.87 ± 0.13
7136 [Ar III]	3.20 ± 0.26	4.86 ± 0.19	5.07 ± 0.19	5.45 ± 0.29	5.40 ± 0.19
7281 He I	...	...	...	...	1.00 ± 0.13
7320 [O II]	...	...	...	1.66 ± 0.20	2.73 ± 0.12
7330 [O II]	...	...	...	1.03 ± 0.21	2.38 ± 0.11
$C(\mathrm{H}\beta)$	0.180	0.145	0.085	0.235	0.090
$F(\mathrm{H}\beta)$[a]	72.00	154.80	260.10	71.57	274.00
$EW(\mathrm{H}\beta)$ Å	84.1	110.9	78.8	75.2	151.7
EW(abs) Å	1.00	2.00	0.00	1.70	0.90
	J1248+4823	J1327+4022	J1331+4151	J1355+4651	J1608+3528
3727 [O II]	82.88 ± 1.46	47.88 ± 1.12	70.05 ± 1.18	28.00 ± 0.76	28.74 ± 1.09
3750 H12	5.95 ± 1.10	4.78 ± 0.75	3.34 ± 0.34	3.34 ± 0.64	2.54 ± 0.88

Table 4. continued.

Ion	$I(\lambda)/I(\mathrm{H}\beta)$	$I(\lambda)/I(\mathrm{H}\beta)$	$I(\lambda)/I(\mathrm{H}\beta)$	$I(\lambda)/I(\mathrm{H}\beta)$	$I(\lambda)/I(\mathrm{H}\beta)$
			Galaxy		
3771 H11	6.38 ± 0.91	4.84 ± 0.71	3.47 ± 0.32	4.27 ± 0.63	5.59 ± 0.83
3798 H10	7.65 ± 0.89	5.46 ± 0.72	5.20 ± 0.31	6.18 ± 0.60	6.68 ± 0.75
3820 He I	1.09 ± 0.22	...	1.00 ± 0.17	...	...
3835 H9	8.61 ± 0.70	8.29 ± 0.75	6.82 ± 0.32	7.66 ± 0.64	8.80 ± 0.72
3868 [Ne III]	47.37 ± 0.84	42.43 ± 0.83	45.76 ± 0.74	48.77 ± 0.93	75.21 ± 1.49
3889 He I + H8	20.72 ± 0.56	19.77 ± 0.75	19.88 ± 0.43	20.41 ± 0.66	22.80 ± 0.86
3968 [Ne III] + H7	30.31 ± 0.65	28.84 ± 0.75	30.21 ± 0.54	30.96 ± 0.73	41.71 ± 1.00
4026 He I	1.68 ± 0.19	1.87 ± 0.21	1.77 ± 0.10	2.23 ± 0.26	2.69 ± 0.34
4068 [S II]	1.40 ± 0.18	...	1.11 ± 0.11	...	...
4101 Hδ	26.60 ± 0.56	26.48 ± 0.69	26.93 ± 0.49	27.26 ± 0.68	29.05 ± 0.78
4340 Hγ	47.17 ± 0.80	49.30 ± 0.92	49.22 ± 0.76	48.74 ± 0.88	48.10 ± 0.98
4363 [O III]	12.87 ± 0.28	13.35 ± 0.32	14.02 ± 0.24	19.51 ± 0.41	21.44 ± 0.53
4387 He I	...	...	0.60 ± 0.08	...	...
4471 He I	3.39 ± 0.18	3.74 ± 0.18	3.86 ± 0.12	3.50 ± 0.24	3.76 ± 0.25
4658 [Fe III]	0.65 ± 0.12	1.25 ± 0.15	0.81 ± 0.11	...	...
4686 He II	1.74 ± 0.14	4.11 ± 0.19	1.95 ± 0.10	2.30 ± 0.18	2.72 ± 0.22
4711 [Ar IV] + He I	1.61 ± 0.12	2.28 ± 0.17	2.19 ± 0.10	3.40 ± 0.18	4.68 ± 0.24
4740 [Ar IV]	0.93 ± 0.10	1.53 ± 0.17	1.50 ± 0.10	2.76 ± 0.17	3.25 ± 0.23
4861 Hβ	100.00 ± 1.53	100.00 ± 1.56	100.00 ± 1.46	100.00 ± 1.57	100.00 ± 1.67
4921 He I	1.00 ± 0.12	1.29 ± 0.14	1.03 ± 0.08	1.78 ± 0.18	1.33 ± 0.17
4959 [O III]	192.98 ± 2.90	181.08 ± 2.72	182.78 ± 2.64	198.21 ± 3.02	261.97 ± 4.13
4988 [Fe III]	1.32 ± 0.16	...	...	...	...
5007 [O III]	574.50 ± 8.58	530.49 ± 7.87	545.93 ± 7.86	591.50 ± 8.88	784.09 ± 12.18
5199 [N I]	0.82 ± 0.14	...	...	...	...
5876 He I	10.35 ± 0.25	10.15 ± 0.26	10.55 ± 0.19	9.32 ± 0.31	11.05 ± 0.38
6300 [O I]	2.10 ± 0.11	1.24 ± 0.15	1.71 ± 0.08	1.04 ± 0.18	...
6312 [S III]	1.53 ± 0.11	1.83 ± 0.15	1.68 ± 0.08	0.84 ± 0.15	...
6363 [O I]	0.83 ± 0.14	...	0.70 ± 0.08	...	...
6563 Hα	278.55 ± 4.54	277.03 ± 4.51	277.18 ± 4.34	273.92 ± 4.54	278.25 ± 4.78
6583 [N II]	3.11 ± 0.18	2.65 ± 0.20	2.49 ± 0.09	1.25 ± 0.24	0.80 ± 0.19
6678 He I	2.42 ± 0.20	2.72 ± 0.20	2.76 ± 0.10	3.15 ± 0.35	2.78 ± 0.32
6717 [S II]	6.97 ± 0.21	5.30 ± 0.22	6.31 ± 0.14	3.38 ± 0.29	1.71 ± 0.26
6731 [S II]	5.13 ± 0.19	3.86 ± 0.21	4.59 ± 0.12	1.51 ± 0.21	1.87 ± 0.26
7065 He I	2.11 ± 0.18	2.76 ± 0.25	2.42 ± 0.10	2.72 ± 0.29	2.61 ± 0.30
7136 [Ar III]	5.94 ± 0.20	4.98 ± 0.28	4.93 ± 0.14	3.25 ± 0.29	2.66 ± 0.29
7281 He I	...	...	0.45 ± 0.06	...	...
7320 [O II]	0.94 ± 0.12	...	0.78 ± 0.07	...	...
7330 [O II]	0.68 ± 0.10	...	0.75 ± 0.06	...	...
$C(\mathrm{H}\beta)$	0.125	0.060	0.135	0.070	0.440
$F(\mathrm{H}\beta)$[a]	77.84	59.91	280.80	48.28	29.84
$EW(\mathrm{H}\beta)$ Å	114.5	220.9	177.6	353.5	367.5
EW(abs) Å	3.10	0.55	0.55	1.55	1.00

[a] In 10^{-16} erg s^{-1} cm^{-2}.

Table 5. Emission line intensities in medium-resolution MMT spectra.

Ion	$I(\lambda)/I(\mathrm{H}\beta)$	$I(\lambda)/I(\mathrm{H}\beta)$	$I(\lambda)/I(\mathrm{H}\beta)$	$I(\lambda)/I(\mathrm{H}\beta)$	$I(\lambda)/I(\mathrm{H}\beta)$
			Galaxy		
	J0810+1837	J0833+2508 No.1	J0833+2508 No.2	J0931+2717 No.1	J0931+2717 No.2
3727 [O II]	333.47 ± 19.68	215.86 ± 4.70	247.67 ± 11.39	222.07 ± 10.10	239.73 ± 10.47
3835 H9	...	9.13 ± 1.41	...	...	...
3868 [Ne III]	26.50 ± 4.32	22.93 ± 1.15	31.27 ± 4.11	12.55 ± 2.46	13.68 ± 2.84
3889 He I + H8	...	20.06 ± 1.38	21.80 ± 4.84	...	23.72 ± 7.27
3968 [Ne III] + H7	...	21.04 ± 1.33	...	...	18.01 ± 6.66
4101 Hδ	30.93 ± 5.14	25.50 ± 1.40	20.12 ± 3.81	33.94 ± 5.02	33.87 ± 4.46
4340 Hγ	52.07 ± 5.28	47.65 ± 1.50	47.62 ± 3.73	45.77 ± 4.31	48.50 ± 3.79
4363 [O III]	4.38 ± 2.49	6.00 ± 0.66	7.32 ± 2.17	...	...
4471 He I	...	3.08 ± 0.67	...	...	...
4861 Hβ	100.00 ± 7.16	100.00 ± 2.21	100.00 ± 4.97	100.00 ± 4.95	100.00 ± 4.78
4959 [O III]	79.84 ± 5.77	98.41 ± 2.11	67.35 ± 3.61	43.64 ± 2.91	51.96 ± 3.23
5007 [O III]	245.45 ± 13.26	279.67 ± 5.35	195.76 ± 7.77	148.64 ± 6.26	171.50 ± 6.88
$C(\mathrm{H}\beta)$	0.000	0.000	0.095	0.000	0.000
$F(\mathrm{H}\beta)$[a]	1.63	11.43	2.54	2.77	2.90
$EW(\mathrm{H}\beta)$ Å	8.4	45.4	24.7	16.5	18.2
EW(abs) Å	2.00	1.10	0.60	2.00	2.00
	DDO68 No.3	DDO68 No.4	J1057+1358 No.1	J1121+3744 No.1	J1231+4205
3727 [O II]	50.62 ± 1.04	94.10 ± 1.70	167.37 ± 12.83	85.87 ± 9.69	217.62 ± 4.75
3750 H12	1.57 ± 0.43	...	...	...	...
3771 H11	2.33 ± 0.48	...	...	...	...
3798 H10	2.92 ± 0.43	...	...	...	...
3835 H9	6.23 ± 0.51	6.92 ± 1.84	...	...	...
3868 [Ne III]	10.07 ± 0.40	6.60 ± 0.56	...	...	19.64 ± 1.00
3889 He I + H8	17.74 ± 0.62	18.13 ± 1.20	...	...	23.11 ± 1.37
3968 [Ne III] + H7	16.35 ± 0.59	15.72 ± 1.13	...	...	18.48 ± 1.27
4101 Hδ	26.73 ± 0.68	25.56 ± 1.14	29.63 ± 18.20	...	25.52 ± 1.32
4340 Hγ	49.34 ± 0.98	47.71 ± 1.27	49.33 ± 12.01	46.79 ± 11.18	47.20 ± 1.52
4363 [O III]	2.82 ± 0.25	1.64 ± 0.38	...	...	4.56 ± 0.46
4471 He I	3.28 ± 0.25	1.38 ± 0.33	...	...	...
4861 Hβ	100.00 ± 1.70	100.00 ± 1.95	100.00 ± 8.43	100.00 ± 10.98	100.00 ± 2.22
4959 [O III]	39.56 ± 0.71	23.79 ± 0.72	16.67 ± 4.03	41.67 ± 6.28	72.33 ± 1.62
5007 [O III]	115.29 ± 1.84	68.36 ± 1.40	61.64 ± 5.78	120.02 ± 10.13	211.63 ± 4.10
$C(\mathrm{H}\beta)$	0.000	0.000	0.000	0.000	0.190
$F(\mathrm{H}\beta)$[a]	21.91	9.20	2.48	1.63	11.09
$EW(\mathrm{H}\beta)$ Å	15.7	36.0	8.7	8.4	65.7
EW(abs) Å	0.00	0.80	2.00	2.00	0.55
	J0834+5905	J0959+4626			
3727 [O II]	133.11 ± 4.64	265.84 ± 7.83			
3750 H12	...	...			
3771 H11	...	...			
3798 H10	...	...			
3835 H9	...	7.94 ± 2.35			
3868 [Ne III]	17.03 ± 2.40	16.41 ± 2.60			
3889 He I + H8	19.20 ± 3.32	17.94 ± 2.82			
3968 [Ne III] + H7	...	...			
4101 Hδ	21.06 ± 3.31	29.73 ± 2.72			
4340 Hγ	47.70 ± 2.57	45.50 ± 2.46			
4363 [O III]	6.26 ± 1.19	...			
4471 He I	...	...			
4861 Hβ	100.00 ± 3.45	100.00 ± 3.19			
4959 [O III]	57.00 ± 2.58	46.00 ± 1.80			
5007 [O III]	164.13 ± 4.76	131.71 ± 3.56			
$C(\mathrm{H}\beta)$	0.010	0.265			
$F(\mathrm{H}\beta)$[a]	4.27	6.88			
$EW(\mathrm{H}\beta)$ Å	28.3	57.0			
EW(abs) Å	0.90	0.00			

[a] In 10^{-16} erg s^{-1} cm^{-2}.

Table 6. Ionic and total heavy element abundances derived from 3.5 m APO spectra.

	Galaxy				
Property	J0113+0052No.1[a]	J0113+0052No.2[a]	J0113+0052No.3[a]	J0113+0052No.4[a]	J0138+0020[b]
T_e(O III) (K)	22427 ± 3086	19102 ± 1032	26186 ± 3779	19007 ± 1010	17131 ± 1110
T_e(O II) (K)	16379 ± 1904	16103 ± 778	15387 ± 1375	16079 ± 764	15427 ± 1343
T_e(S III) (K)	20314 ± 2561	17555 ± 857	23435 ± 3136	17476 ± 838	15919 ± 922
O^+/H^+ ($\times10^4$)	0.058 ± 0.017	0.146 ± 0.020	0.128 ± 0.030	0.062 ± 0.008	0.187 ± 0.049
O^{++}/H^+ ($\times10^4$)	0.085 ± 0.025	0.063 ± 0.008	0.071 ± 0.021	0.121 ± 0.015	0.144 ± 0.025
O^{+++}/H^+ ($\times10^6$)	...	...	...	...	...
O/H ($\times10^4$)	0.142 ± 0.030	0.209 ± 0.021	0.199 ± 0.037	0.183 ± 0.017	0.331 ± 0.055
12 + log(O/H)	7.153 ± 0.093	7.320 ± 0.044	7.300 ± 0.081	7.263 ± 0.041	7.519 ± 0.073
N^+/H^+ ($\times10^6$)	...	0.485 ± 0.064	...	0.228 ± 0.027	...
ICF	...	1.364	...	2.960	...
log(N/O)	...	−1.500 ± 0.075	...	−1.434 ± 0.066	...
Ne^{++}/H^+ ($\times10^5$)	0.233 ± 0.070	...	...	...	...
ICF	1.158	...	...	...	...
log(Ne/O)	−0.722 ± 0.211	...	...	...	...
S^+/H^+ ($\times10^6$)	...	0.294 ± 0.026	0.213 ± 0.030	...	...
S^{++}/H^+ ($\times10^6$)	...	...	...	...	...
ICF	...	...	...	...	...
log(S/O)	...	...	...	...	...
Cl^{++}/H^+ ($\times10^8$)	...	...	...	...	...
ICF	...	...	...	...	...
log(Cl/O)	...	...	...	...	...
Ar^{++}/H^+ ($\times10^7$)	...	...	...	...	...
Ar^{+++}/H^+ ($\times10^7$)	...	...	...	...	...
ICF	...	...	...	...	...
log(Ar/O)	...	...	...	...	...
Fe^{++}/H^+($\times10^6$)(4658)	...	...	...	...	...
Fe^{++}/H^+($\times10^6$)(4988)	...	...	...	...	...
ICF	...	...	...	...	...
log(Fe/O) (λ4658)	...	...	...	...	...
log(Fe/O) (4988)	...	...	...	...	...
Property	J0834+5905No.1[b]	J0834+5905No.2[b]	J0843+4025[b]	J0851+8416[a]	J0906+2528No.1[a]
T_e(O III) (K)	17777 ± 1017	18422 ± 1068	16763 ± 1018	15138 ± 1115	18185 ± 3407
T_e(O II) (K)	15691 ± 1242	15913 ± 1318	15259 ± 1224	14357 ± 968	15836 ± 2671
T_e(S III) (K)	16455 ± 844	16990 ± 886	15613 ± 845	14747 ± 926	16794 ± 2828
O^+/H^+ ($\times10^4$)	0.124 ± 0.026	0.134 ± 0.031	0.226 ± 0.048	0.122 ± 0.023	0.201 ± 0.084
O^{++}/H^+ ($\times10^4$)	0.143 ± 0.020	0.100 ± 0.015	0.147 ± 0.022	0.335 ± 0.064	0.116 ± 0.051
O^{+++}/H^+ ($\times10^6$)	...	...	...	...	...
O/H ($\times10^4$)	0.267 ± 0.033	0.235 ± 0.035	0.373 ± 0.053	0.457 ± 0.068	0.317 ± 0.098
12 + log(O/H)	7.427 ± 0.053	7.370 ± 0.064	7.572 ± 0.062	7.660 ± 0.064	7.502 ± 0.135
N^+/H^+ ($\times10^6$)	0.400 ± 0.076	...	0.607 ± 0.109	0.421 ± 0.049	0.347 ± 0.105
ICF	2.173	...	1.620	3.713	1.537
log(N/O)	−1.487 ± 0.098	...	−1.579 ± 0.101	−1.466 ± 0.094	−1.774 ± 0.190
Ne^{++}/H^+ ($\times10^5$)	...	...	...	0.497 ± 0.109	0.283 ± 0.127
ICF	...	...	...	1.092	1.305
log(Ne/O)	...	...	...	−0.925 ± 0.135	−0.934 ± 0.428
S^+/H^+ ($\times10^6$)	0.206 ± 0.028	0.458 ± 0.070	0.420 ± 0.053	0.162 ± 0.018	0.391 ± 0.092
S^{++}/H^+ ($\times10^6$)	...	...	...	...	...
ICF	...	...	...	...	...
log(S/O)	...	...	...	...	...
Cl^{++}/H^+ ($\times10^8$)	...	...	...	...	...
ICF	...	...	...	...	...
log(Cl/O)	...	...	...	...	...
Ar^{++}/H^+ ($\times10^7$)	...	...	...	...	...

Table 6. continued.

	Galaxy				
Ar^{+++}/H^+ ($\times10^7$)	...	...	...	...	...
ICF	...	...	...	...	...
log(Ar/O)	...	...	...	...	...
Fe^{++}/H^+($\times10^6$)(4658)	...	...	...	...	...
Fe^{++}/H^+($\times10^6$)(4988)	...	...	...	...	...
ICF	...	...	...	...	...
log(Fe/O) (λ4658)	...	...	...	...	...
log(Fe/O) (4988)	...	...	...	...	...
Property	J0906+2528No.2[a]	J0908+0517No.1[b]	J0908+0517No.2[a]	J0950+3127No.1[b]	J0950+3127No.2[a]
T_e(O III) (K)	16859 ± 1865	18467 ± 1146	16151 ± 478	18248 ± 1099	19018 ± 4780
T_e(O II) (K)	15304 ± 1535	15927 ± 1416	14950 ± 403	15857 ± 1352	16082 ± 3616
T_e(S III) (K)	15693 ± 1548	17028 ± 951	15105 ± 397	16846 ± 912	17485 ± 3967
O^+/H^+ ($\times10^4$)	0.105 ± 0.028	0.174 ± 0.046	0.082 ± 0.006	0.168 ± 0.041	0.149 ± 0.082
O^{++}/H^+ ($\times10^4$)	0.186 ± 0.050	0.072 ± 0.012	0.374 ± 0.028	0.086 ± 0.014	0.132 ± 0.077
O^{+++}/H^+ ($\times10^6$)	...	...	2.190 ± 0.301	...	...
O/H ($\times10^4$)	0.291 ± 0.058	0.245 ± 0.047	0.478 ± 0.029	0.254 ± 0.043	0.281 ± 0.112
12 + log(O/H)	7.464 ± 0.086	7.390 ± 0.083	7.680 ± 0.026	7.405 ± 0.073	7.448 ± 0.174
N^+/H^+ ($\times10^6$)	0.390 ± 0.075	0.633 ± 0.166	0.401 ± 0.025	...	0.359 ± 0.153
ICF	2.800	1.335	5.643	...	1.889
log(N/O)	−1.426 ± 0.119	−1.463 ± 0.146	−1.324 ± 0.038	...	−1.617 ± 0.254
Ne^{++}/H^+ ($\times10^5$)	0.401 ± 0.138	...	0.776 ± 0.065	...	...
ICF	1.135	...	1.072	...	...
log(Ne/O)	−0.806 ± 0.223	...	−0.759 ± 0.051	...	...
S^+/H^+ ($\times10^6$)	0.133 ± 0.021	0.439 ± 0.072	0.229 ± 0.010	...	0.253 ± 0.080
S^{++}/H^+ ($\times10^6$)	...	...	0.846 ± 0.132	...	...
ICF	...	...	1.457	...	...
log(S/O)	...	...	−1.485 ± 0.060	...	...
Cl^{++}/H^+ ($\times10^8$)	...	...	...	...	...
ICF	...	...	...	...	...
log(Cl/O)	...	...	...	...	...
Ar^{++}/H^+ ($\times10^7$)	...	...	2.302 ± 0.139	...	2.463 ± 0.774
Ar^{+++}/H^+ ($\times10^7$)	...	...	...	...	...
ICF	...	...	1.402	...	1.044
log(Ar/O)	...	...	−2.171 ± 0.037	...	−2.038 ± 0.221
Fe^{++}/H^+($\times10^6$)(4658)	...	...	...	...	...
Fe^{++}/H^+($\times10^6$)(4988)	...	...	...	...	...
ICF	...	...	...	...	...
log(Fe/O) (λ4658)	...	...	...	...	...
log(Fe/O) (4988)	...	...	...	...	...
Property	DDO68 No.2[a]	DDO68 No.3[a]	J1056+3608No.1[a]	J1056+3608No.2[a]	J1056+3608No.3[a]
T_e(O III) (K)	17046 ± 1043	17069 ± 2053	22610 ± 2410	25776 ± 6755	20945 ± 3381
T_e(O II) (K)	15389 ± 853	15400 ± 1678	16363 ± 1464	15563 ± 2713	16390 ± 2313
T_e(S III) (K)	15848 ± 865	15867 ± 1704	20467 ± 2000	23094 ± 5606	19084 ± 2806
O^+/H^+ ($\times10^4$)	0.038 ± 0.006	0.048 ± 0.014	0.053 ± 0.012	0.158 ± 0.070	0.116 ± 0.040
O^{++}/H^+ ($\times10^4$)	0.112 ± 0.017	0.073 ± 0.021	0.090 ± 0.021	0.049 ± 0.026	0.086 ± 0.031
O^{+++}/H^+ ($\times10^6$)	...	...	...	...	...
O/H ($\times10^4$)	0.150 ± 0.018	0.121 ± 0.025	0.143 ± 0.024	0.207 ± 0.075	0.202 ± 0.050
12 + log(O/H)	7.176 ± 0.051	7.083 ± 0.090	7.155 ± 0.073	7.316 ± 0.157	7.306 ± 0.108
N^+/H^+ ($\times10^6$)	...	...	0.187 ± 0.040	0.589 ± 0.186	0.411 ± 0.108
ICF	...	...	2.723	1.199	1.717
log(N/O)	...	...	−1.448 ± 0.117	−1.467 ± 0.217	−1.457 ± 0.158
Ne^{++}/H^+ ($\times10^5$)	0.227 ± 0.038	0.124 ± 0.039	0.188 ± 0.049	...	0.319 ± 0.117
ICF	1.086	1.155	1.140	...	1.264
log(Ne/O)	−0.785 ± 0.103	−0.928 ± 0.218	−0.825 ± 0.173	...	−0.700 ± 0.315

Table 6. continued.

	Galaxy				
S^+/H^+ ($\times10^6$)	0.084 ± 0.007	0.067 ± 0.011	0.088 ± 0.014	0.235 ± 0.060	0.185 ± 0.037
S^{++}/H^+ ($\times10^6$)	...	...	...	...	...
ICF	...	...	...	...	...
log(S/O)	...	...	...	...	...
Cl^{++}/H^+ ($\times10^8$)	...	...	...	...	...
ICF	...	...	...	...	...
log(Cl/O)	...	...	...	...	...
Ar^{++}/H^+ ($\times10^7$)	0.673 ± 0.075	...	...	...	...
Ar^{+++}/H^+ ($\times10^7$)	...	...	...	...	...
ICF	1.173	...	...	...	...
log(Ar/O)	−2.279 ± 0.070	...	...	...	...
Fe^{++}/H^+($\times10^6$)(4658)	...	...	...	...	...
Fe^{++}/H^+($\times10^6$)(4988)	...	...	...	...	...
ICF	...	...	...	...	...
log(Fe/O) (λ4658)	...	...	...	...	...
log(Fe/O) (4988)	...	...	...	...	...
Property	J1109+2007[a]	J1119+0935No.1[b]	J1119+0935No.2[a]	J1119+0935No.3[b]	J1121+3744No.1[b]
T_e(O III) (K)	24617 ± 3823	17349 ± 1010	13998 ± 899	18231 ± 1151	20000 ± 1817
T_e(O II) (K)	15969 ± 1875	15521 ± 1226	13570 ± 803	15851 ± 1417	16284 ± 2304
T_e(S III) (K)	22132 ± 3173	16100 ± 838	13784 ± 746	16832 ± 955	18300 ± 1508
O^+/H^+ ($\times10^4$)	0.207 ± 0.060	0.124 ± 0.025	0.196 ± 0.034	0.220 ± 0.056	0.025 ± 0.018
O^{++}/H^+ ($\times10^4$)	0.085 ± 0.028	0.173 ± 0.025	0.310 ± 0.054	0.052 ± 0.009	0.034 ± 0.011
O^{+++}/H^+ ($\times10^6$)	...	...	...	...	...
O/H ($\times10^4$)	0.292 ± 0.066	0.296 ± 0.035	0.506 ± 0.064	0.272 ± 0.057	0.060 ± 0.021
12 + log(O/H)	7.466 ± 0.099	7.472 ± 0.052	7.704 ± 0.055	7.434 ± 0.090	6.776 ± 0.155
N^+/H^+ ($\times10^6$)	0.373 ± 0.085	0.458 ± 0.078	0.636 ± 0.075	0.888 ± 0.141	...
ICF	1.333	2.421	2.608	1.102	...
log(N/O)	−1.768 ± 0.144	−1.427 ± 0.089	−1.485 ± 0.075	−1.442 ± 0.172	...
Ne^{++}/H^+ ($\times10^5$)	...	...	0.589 ± 0.117	...	...
ICF	...	...	1.148	...	...
log(Ne/O)	...	...	−0.874 ± 0.134	...	...
S^+/H^+ ($\times10^6$)	0.325 ± 0.054	0.321 ± 0.039	0.336 ± 0.033	...	...
S^{++}/H^+ ($\times10^6$)	...	...	...	...	...
ICF	...	...	...	...	...
log(S/O)	...	...	...	...	...
Cl^{++}/H^+ ($\times10^8$)	...	...	...	...	...
ICF	...	...	...	...	...
log(Cl/O)	...	...	...	...	...
Ar^{++}/H^+ ($\times10^7$)	...	0.915 ± 0.244	1.620 ± 0.184	...	...
Ar^{+++}/H^+ ($\times10^7$)	...	...	...	...	...
ICF	...	1.046	1.054	...	...
log(Ar/O)	...	−2.491 ± 0.127	−2.472 ± 0.074	...	...
Fe^{++}/H^+($\times10^6$)(4658)	...	...	...	...	...
Fe^{++}/H^+($\times10^6$)(4988)	...	...	...	...	...
ICF	...	...	...	...	...
log(Fe/O) (λ4658)	...	...	...	...	...
log(Fe/O) (4988)	...	...	...	...	...
Property	J1146+4050[b]	J1226-0115No.1[a]	J1226-0115No.2[a]	J1235+2755No.1[a]	J1235+2755No.2[a]
T_e(O III) (K)	18792 ± 1032	16214 ± 267	15109 ± 240	16555 ± 1006	14042 ± 360
T_e(O II) (K)	16021 ± 1282	14983 ± 224	14339 ± 208	15158 ± 836	13603 ± 321
T_e(S III) (K)	17297 ± 856	15158 ± 221	14724 ± 199	15441 ± 835	13823 ± 299
O^+/H^+ ($\times10^4$)	0.142 ± 0.030	0.086 ± 0.004	0.091 ± 0.004	0.183 ± 0.027	0.235 ± 0.016
O^{++}/H^+ ($\times10^4$)	0.078 ± 0.011	0.507 ± 0.022	0.551 ± 0.024	0.197 ± 0.030	0.445 ± 0.031

Table 6. continued.

	Galaxy				
O^{+++}/H^+ ($\times10^6$)	...	...	0.925 ± 0.127	...	...
O/H ($\times10^4$)	0.220 ± 0.031	0.593 ± 0.022	0.652 ± 0.024	0.380 ± 0.040	0.680 ± 0.035
12 + log(O/H)	7.343 ± 0.062	7.773 ± 0.016	7.814 ± 0.016	7.579 ± 0.046	7.832 ± 0.023
N^+/H^+ ($\times10^6$)	0.727 ± 0.129	0.328 ± 0.011	0.406 ± 0.013	0.329 ± 0.040	0.715 ± 0.035
ICF	1.502	6.637	6.836	2.088	2.919
log(N/O)	−1.305 ± 0.101	−1.435 ± 0.022	−1.370 ± 0.022	−1.743 ± 0.070	−1.513 ± 0.031
Ne^{++}/H^+ ($\times10^5$)	...	0.948 ± 0.044	0.922 ± 0.045	0.474 ± 0.087	1.051 ± 0.082
ICF	...	1.047	1.050	1.203	1.127
log(Ne/O)	...	−0.776 ± 0.028	−0.828 ± 0.029	−0.824 ± 0.135	−0.759 ± 0.051
S^+/H^+ ($\times10^6$)	0.298 ± 0.039	0.210 ± 0.018	0.179 ± 0.005	0.185 ± 0.024	0.257 ± 0.011
S^{++}/H^+ ($\times10^6$)	...	0.770 ± 0.055	0.923 ± 0.062	...	0.834 ± 0.112
ICF	...	1.618	1.651	...	1.033
log(S/O)	...	−1.593 ± 0.030	−1.554 ± 0.029	...	−1.780 ± 0.050
Cl^{++}/H^+ ($\times10^8$)	...	...	...	...	...
ICF	...	...	...	...	...
log(Cl/O)	...	...	...	...	...
Ar^{++}/H^+ ($\times10^7$)	1.257 ± 0.482	2.428 ± 0.076	2.197 ± 0.067	...	2.390 ± 0.110
Ar^{+++}/H^+ ($\times10^7$)	...	0.817 ± 0.131	0.923 ± 0.185	...	...
ICF	1.070	1.551	1.582	...	1.073
log(Ar/O)	−2.214 ± 0.178	−2.197 ± 0.032	−2.273 ± 0.042	...	−2.423 ± 0.030
Fe^{++}/H^+($\times10^6$)(4658)	...	...	...	...	...
Fe^{++}/H^+($\times10^6$)(4988)	...	...	...	...	...
ICF	...	...	...	...	...
log(Fe/O) (λ4658)	...	...	...	...	...
log(Fe/O) (4988)	...	...	...	...	...
Property	J1235+2755No.3[a]	J1241-0340[a]	J1257+3341No.1[a]	J1257+3341No.2[b]	J1257+3341No.3[a]
T_e(O III) (K)	15450 ± 539	16545 ± 246	15895 ± 2193	16413 ± 1028	17022 ± 2091
T_e(O II) (K)	14551 ± 464	15153 ± 204	14810 ± 1862	15087 ± 1230	15379 ± 1712
T_e(S III) (K)	15000 ± 448	15432 ± 204	14893 ± 1821	15323 ± 854	15828 ± 1735
O^+/H^+ ($\times10^4$)	0.233 ± 0.021	0.113 ± 0.004	0.144 ± 0.048	0.269 ± 0.059	0.173 ± 0.049
O^{++}/H^+ ($\times10^4$)	0.358 ± 0.032	0.436 ± 0.017	0.151 ± 0.052	0.147 ± 0.023	0.128 ± 0.038
O^{+++}/H^+ ($\times10^6$)	...	...	...	...	...
O/H ($\times10^4$)	0.591 ± 0.038	0.548 ± 0.017	0.295 ± 0.071	0.416 ± 0.064	0.301 ± 0.062
12 + log(O/H)	7.772 ± 0.028	7.739 ± 0.014	7.470 ± 0.105	7.619 ± 0.067	7.479 ± 0.090
N^+/H^+ ($\times10^6$)	0.695 ± 0.043	0.330 ± 0.010	0.525 ± 0.123	...	0.536 ± 0.071
ICF	2.559	4.767	2.055	...	1.722
log(N/O)	−1.522 ± 0.039	−1.542 ± 0.019	−1.437 ± 0.146	...	−1.537 ± 0.128
Ne^{++}/H^+ ($\times10^5$)	0.846 ± 0.084	1.051 ± 0.043	0.364 ± 0.132	0.822 ± 0.179	0.315 ± 0.100
ICF	1.153	1.067	1.207	1.316	1.263
log(Ne/O)	−0.783 ± 0.068	−0.689 ± 0.025	−0.827 ± 0.276	−0.585 ± 0.214	−0.880 ± 0.273
S^+/H^+ ($\times10^6$)	0.240 ± 0.012	0.166 ± 0.004	0.227 ± 0.043	...	0.172 ± 0.029
S^{++}/H^+ ($\times10^6$)	0.724 ± 0.095	0.795 ± 0.057	...	...	...
ICF	0.982	1.317	...	...	...
log(S/O)	−1.796 ± 0.052	−1.637 ± 0.029	...	...	...
Cl^{++}/H^+ ($\times10^8$)	...	...	...	...	...
ICF	...	...	...	...	...
log(Cl/O)	...	...	...	...	...
Ar^{++}/H^+ ($\times10^7$)	2.367 ± 0.125	2.277 ± 0.063	0.879 ± 0.232	...	1.028 ± 0.239
Ar^{+++}/H^+ ($\times10^7$)	...	...	...	...	...
ICF	1.051	1.279	1.041	...	1.052
log(Ar/O)	−2.376 ± 0.036	−2.274 ± 0.018	−2.508 ± 0.155	...	−2.445 ± 0.135
Fe^{++}/H^+($\times10^6$)(4658)	...	...	...	...	...
Fe^{++}/H^+($\times10^6$)(4988)	...	...	...	...	...

Table 6. continued.

	Galaxy				
ICF	...	...	...	...	...
log(Fe/O) (λ4658)	...	...	...	...	...
log(Fe/O) (4988)	...	...	...	...	...
Property	J1403+5804No.1[b]	J1403+5804No.2[a]	SBS 1420+544[a]	PHL293B[a]	
T_e(O III) (K)	18535 ± 1034	19766 ± 1341	16600 ± 262	17172 ± 320	
T_e(O II) (K)	15947 ± 1279	16244 ± 979	15180 ± 218	15445 ± 260	
T_e(S III) (K)	17084 ± 858	18106 ± 1113	15478 ± 218	15952 ± 265	
O^+/H^+ ($\times10^4$)	0.124 ± 0.027	0.086 ± 0.013	0.050 ± 0.002	0.090 ± 0.004	
O^{++}/H^+ ($\times10^4$)	0.104 ± 0.014	0.165 ± 0.026	0.569 ± 0.023	0.371 ± 0.017	
O^{+++}/H^+ ($\times10^6$)	...	...	...	0.414 ± 0.072	
O/H ($\times10^4$)	0.228 ± 0.030	0.251 ± 0.029	0.619 ± 0.023	0.465 ± 0.018	
12 + log(O/H)	7.358 ± 0.057	7.400 ± 0.049	7.792 ± 0.016	7.667 ± 0.017	
N^+/H^+ ($\times10^6$)	0.406 ± 0.097	0.197 ± 0.029	0.158 ± 0.008	0.147 ± 0.007	
ICF	1.839	2.936	11.432	5.034	
log(N/O)	−1.485 ± 0.119	−1.639 ± 0.080	−1.536 ± 0.029	−1.797 ± 0.028	
Ne^{++}/H^+ ($\times10^5$)	...	0.361 ± 0.059	1.216 ± 0.054	0.875 ± 0.044	
ICF	...	1.126	1.029	1.066	
log(Ne/O)	...	−0.791 ± 0.108	−0.694 ± 0.026	−0.697 ± 0.031	
S^+/H^+ ($\times10^6$)	0.208 ± 0.038	0.122 ± 0.012	0.084 ± 0.003	0.110 ± 0.004	
S^{++}/H^+ ($\times10^6$)	...	...	0.550 ± 0.062	0.455 ± 0.063	
ICF	...	...	2.408	1.359	
log(S/O)	...	...	−1.608 ± 0.046	−1.782 ± 0.051	
Cl^{++}/H^+ ($\times10^8$)	...	...	...	...	
ICF	...	...	...	...	
log(Cl/O)	...	...	...	...	
Ar^{++}/H^+ ($\times10^7$)	...	1.008 ± 0.150	1.663 ± 0.064	1.396 ± 0.055	
Ar^{+++}/H^+ ($\times10^7$)	...	...	1.309 ± 0.193	0.774 ± 0.136	
ICF	...	1.075	2.323	1.315	
log(Ar/O)	...	−2.365 ± 0.081	−2.205 ± 0.056	−2.404 ± 0.049	
Fe^{++}/H^+($\times10^6$)(4658)	...	...	...	0.178 ± 0.027	
Fe^{++}/H^+($\times10^6$)(4988)	...	...	...	...	
ICF	...	...	...	7.060	
log(Fe/O) (λ4658)	...	...	...	−1.569 ± 0.067	
log(Fe/O) (4988)	...	...	...	...	

[a] Direct method. [b] Semi-empirical method.

Table 7. Ionic and total heavy element abundances derived from the low-resolution MMT spectra.

	Galaxy				
Property	J1016+3754[a]	J1016+5823No.1[a]	J1016+5823No.2[a]	J1016+5823No.3[a]	J1044+0353[a]
T_e(O III) (K)	17167 ± 214	15410 ± 205	15170 ± 1093	16960 ± 265	19881 ± 256
T_e(O II) (K)	15443 ± 174	14526 ± 177	14377 ± 947	15351 ± 217	16265 ± 186
T_e(S III) (K)	15949 ± 178	14968 ± 170	14774 ± 907	15776 ± 220	18201 ± 212
O^+/H^+ ($\times10^4$)	0.052 ± 0.002	0.115 ± 0.004	0.139 ± 0.026	0.088 ± 0.004	0.024 ± 0.001
O^{++}/H^+ ($\times10^4$)	0.373 ± 0.012	0.422 ± 0.015	0.253 ± 0.047	0.327 ± 0.013	0.247 ± 0.008
O^{+++}/H^+ ($\times10^6$)	1.490 ± 0.125	0.741 ± 0.111	...	0.362 ± 0.079	0.587 ± 0.040
O/H ($\times10^4$)	0.441 ± 0.012	0.545 ± 0.016	0.393 ± 0.054	0.418 ± 0.014	0.277 ± 0.008
12 + log(O/H)	7.644 ± 0.012	7.736 ± 0.013	7.594 ± 0.059	7.622 ± 0.014	7.442 ± 0.012
N^+/H^+ ($\times10^6$)	0.157 ± 0.008	0.230 ± 0.010	0.514 ± 0.067	0.172 ± 0.011	0.063 ± 0.004
ICF	7.976	4.649	2.840	4.670	10.950
log(N/O)	−1.545 ± 0.026	−1.707 ± 0.024	−1.430 ± 0.082	−1.717 ± 0.031	−1.605 ± 0.032
Ne^{++}/H^+ ($\times10^5$)	0.725 ± 0.025	0.865 ± 0.034	0.456 ± 0.097	0.660 ± 0.029	0.471 ± 0.015
ICF	1.049	1.074	1.132	1.072	1.035
log(Ne/O)	−0.763 ± 0.021	−0.768 ± 0.024	−0.882 ± 0.139	−0.772 ± 0.026	−0.754 ± 0.019
S^+/H^+ ($\times10^6$)	0.077 ± 0.002	0.151 ± 0.004	0.310 ± 0.033	0.122 ± 0.004	0.039 ± 0.001
S^{++}/H^+ ($\times10^6$)	0.650 ± 0.050	0.725 ± 0.067	...	0.348 ± 0.068	0.233 ± 0.024
ICF	1.837	1.298	...	1.302	2.328
log(S/O)	−1.518 ± 0.032	−1.680 ± 0.035	...	−1.835 ± 0.065	−1.640 ± 0.041
Cl^{++}/H^+ ($\times10^8$)	...	...	...	...	...
ICF	...	...	...	...	...
log(Cl/O)	...	...	...	...	...
Ar^{++}/H^+ ($\times10^7$)	1.382 ± 0.066	1.259 ± 0.074	...	1.096 ± 0.099	0.667 ± 0.032
Ar^{+++}/H^+ ($\times10^7$)	0.983 ± 0.111	...	...	...	0.561 ± 0.042
ICF	1.760	1.263	...	1.266	2.244
log(Ar/O)	−2.258 ± 0.043	−2.535 ± 0.028	...	−2.480 ± 0.042	−2.267 ± 0.036
Fe^{++}/H^+($\times10^6$)(4658)	0.195 ± 0.028	0.151 ± 0.029	...	0.174 ± 0.034	...
Fe^{++}/H^+($\times10^6$)(4988)	...	0.175 ± 0.018	...	0.240 ± 0.025	...
ICF	11.599	6.475	...	6.507	...
log(Fe/O) (λ4658)	−1.290 ± 0.063	−1.747 ± 0.084	...	−1.568 ± 0.086	...
log(Fe/O) (4988)	...	−1.682 ± 0.046	...	−1.429 ± 0.047	...
Property	J1119+5130[a]	J1132+5722No.1[a]	J1132+5722No.2[a]	J1132+5722No.3[a]	J1154+4636[a]
T_e(O III) (K)	17000 ± 473	15826 ± 511	14711 ± 507	16725 ± 1052	15256 ± 372
T_e(O II) (K)	15369 ± 387	14771 ± 434	14078 ± 445	15241 ± 870	14432 ± 321
T_e(S III) (K)	15810 ± 393	14836 ± 424	14394 ± 421	15582 ± 873	14844 ± 308
O^+/H^+ ($\times10^4$)	0.087 ± 0.006	0.107 ± 0.009	0.155 ± 0.014	0.125 ± 0.019	0.143 ± 0.009
O^{++}/H^+ ($\times10^4$)	0.219 ± 0.015	0.202 ± 0.017	0.389 ± 0.036	0.350 ± 0.054	0.404 ± 0.026
O^{+++}/H^+ ($\times10^6$)	1.428 ± 0.408	0.571 ± 0.108	...	...	1.682 ± 0.305
O/H ($\times10^4$)	0.320 ± 0.017	0.315 ± 0.019	0.544 ± 0.039	0.475 ± 0.058	0.563 ± 0.027
12 + log(O/H)	7.505 ± 0.023	7.498 ± 0.026	7.736 ± 0.031	7.676 ± 0.053	7.751 ± 0.021
N^+/H^+ ($\times10^6$)	0.201 ± 0.017	0.296 ± 0.023	0.649 ± 0.048	0.461 ± 0.078	0.612 ± 0.034
ICF	3.667	2.952	3.502	3.778	3.911
log(N/O)	−1.638 ± 0.044	−1.557 ± 0.041	−1.380 ± 0.045	−1.436 ± 0.091	−1.372 ± 0.032
Ne^{++}/H^+ ($\times10^5$)	0.479 ± 0.036	0.409 ± 0.036	0.579 ± 0.063	0.603 ± 0.106	0.907 ± 0.063
ICF	1.113	1.134	1.099	1.090	1.099
log(Ne/O)	−0.778 ± 0.048	−0.832 ± 0.059	−0.932 ± 0.067	−0.859 ± 0.109	−0.752 ± 0.044
S^+/H^+ ($\times10^6$)	0.123 ± 0.007	0.234 ± 0.011	0.308 ± 0.017	0.240 ± 0.025	0.309 ± 0.013
S^{++}/H^+ ($\times10^6$)	0.447 ± 0.142	0.585 ± 0.101	0.805 ± 0.182	...	1.015 ± 0.138
ICF	1.145	1.038	1.120	...	1.183
log(S/O)	−1.690 ± 0.111	−1.569 ± 0.060	−1.640 ± 0.078	...	−1.556 ± 0.050
Cl^{++}/H^+ ($\times10^8$)	...	...	...	...	...
ICF	...	...	...	...	...
log(Cl/O)	...	...	...	...	...

Table 7. continued.

			Galaxy		
Ar^{++}/H^+ ($\times10^7$)	0.702 ± 0.102	1.086 ± 0.121	2.030 ± 0.207	...	1.816 ± 0.154
Ar^{+++}/H^+ ($\times10^7$)	...	...	...	...	...
ICF	1.143	1.076	1.126	...	1.171
log(Ar/O)	−2.601 ± 0.067	−2.431 ± 0.055	−2.377 ± 0.054	...	−2.423 ± 0.043
Fe^{++}/H^+($\times10^6$)(4658)	...	...	...	...	0.327 ± 0.055
Fe^{++}/H^+($\times10^6$)(4988)	0.188 ± 0.038	0.278 ± 0.035	...	...	0.490 ± 0.067
ICF	4.999	3.954	...	...	5.363
log(Fe/O) (λ4658)	...	...	...	...	−1.507 ± 0.076
log(Fe/O) (4988)	−1.531 ± 0.090	−1.456 ± 0.060	...	...	−1.332 ± 0.063
Property	J1215+5223[a]	J1224+3724[a]	J1244+3212No.1[a]	J1244+3212No.2[a]	J1244+3212No.3[a]
T_e(O III) (K)	16226 ± 401	16288 ± 198	14734 ± 198	14010 ± 295	14238 ± 185
T_e(O II) (K)	14990 ± 337	15022 ± 166	14093 ± 174	13579 ± 264	13746 ± 165
T_e(S III) (K)	15168 ± 333	15219 ± 164	14414 ± 165	13794 ± 245	13992 ± 154
O^+/H^+ ($\times10^4$)	0.100 ± 0.006	0.085 ± 0.003	0.218 ± 0.008	0.212 ± 0.013	0.240 ± 0.009
O^{++}/H^+ ($\times10^4$)	0.238 ± 0.015	0.503 ± 0.016	0.424 ± 0.016	0.587 ± 0.034	0.400 ± 0.015
O^{+++}/H^+ ($\times10^6$)	...	0.755 ± 0.087	0.651 ± 0.126	...	...
O/H ($\times10^4$)	0.338 ± 0.016	0.596 ± 0.017	0.648 ± 0.018	0.799 ± 0.036	0.640 ± 0.017
12 + log(O/H)	7.529 ± 0.021	7.775 ± 0.012	7.812 ± 0.012	7.903 ± 0.020	7.806 ± 0.012
N^+/H^+ ($\times10^6$)	0.275 ± 0.018	0.364 ± 0.013	0.496 ± 0.015	0.469 ± 0.023	0.647 ± 0.019
ICF	3.387	6.715	2.994	3.746	2.694
log(N/O)	−1.561 ± 0.035	−1.387 ± 0.020	−1.640 ± 0.018	−1.658 ± 0.029	−1.565 ± 0.017
Ne^{++}/H^+ ($\times10^5$)	0.486 ± 0.033	0.995 ± 0.035	0.916 ± 0.037	1.132 ± 0.073	0.808 ± 0.033
ICF	1.104	1.050	1.128	1.091	1.142
log(Ne/O)	−0.800 ± 0.043	−0.756 ± 0.021	−0.797 ± 0.027	−0.811 ± 0.040	−0.841 ± 0.027
S^+/H^+ ($\times10^6$)	0.098 ± 0.005	0.140 ± 0.004	0.259 ± 0.006	0.246 ± 0.010	0.282 ± 0.007
S^{++}/H^+ ($\times10^6$)	0.630 ± 0.120	0.681 ± 0.063	0.742 ± 0.065	1.107 ± 0.142	0.902 ± 0.068
ICF	1.102	1.631	1.044	1.157	1.001
log(S/O)	−1.625 ± 0.075	−1.649 ± 0.036	−1.793 ± 0.031	−1.708 ± 0.050	−1.732 ± 0.028
Cl^{++}/H^+ ($\times10^8$)	...	2.159 ± 0.053	...	...	...
ICF	...	1.227	...	...	...
log(Cl/O)	...	−3.352 ± 0.016	...	...	...
Ar^{++}/H^+ ($\times10^7$)	1.259 ± 0.107	1.898 ± 0.077	2.183 ± 0.088	2.546 ± 0.151	2.453 ± 0.095
Ar^{+++}/H^+ ($\times10^7$)	...	1.026 ± 0.097	...	...	...
ICF	1.114	1.563	1.079	1.152	1.059
log(Ar/O)	−2.382 ± 0.043	−2.303 ± 0.031	−2.439 ± 0.021	−2.435 ± 0.032	−2.392 ± 0.021
Fe^{++}/H^+($\times10^6$)(4658)	...	0.170 ± 0.022	0.130 ± 0.033	...	0.163 ± 0.021
Fe^{++}/H^+($\times10^6$)(4988)	...	0.248 ± 0.022	...	...	...
ICF	...	9.645	4.014	...	3.586
log(Fe/O) (λ4658)	...	−1.560 ± 0.058	−2.096 ± 0.110	...	−2.040 ± 0.058
log(Fe/O) (4988)	...	−1.396 ± 0.041	...	...	...
Property	J1248+4823[a]	J1327+4022[a]	J1331+4151[a]	J1355+4651[a]	J1608+3528[a]
T_e(O III) (K)	16052 ± 195	16970 ± 234	17192 ± 183	19749 ± 287	17754 ± 265
T_e(O II) (K)	14896 ± 165	15355 ± 192	15454 ± 149	16241 ± 210	15682 ± 211
T_e(S III) (K)	15023 ± 162	15785 ± 194	15969 ± 152	18092 ± 238	16436 ± 220
O^+/H^+ ($\times10^4$)	0.077 ± 0.003	0.041 ± 0.002	0.058 ± 0.002	0.020 ± 0.001	0.025 ± 0.001
O^{++}/H^+ ($\times10^4$)	0.536 ± 0.017	0.436 ± 0.015	0.433 ± 0.012	0.347 ± 0.012	0.578 ± 0.022
O^{+++}/H^+ ($\times10^6$)	1.260 ± 0.143	2.083 ± 0.186	0.989 ± 0.064	0.945 ± 0.149	1.729 ± 0.244
O/H ($\times10^4$)	0.626 ± 0.018	0.497 ± 0.016	0.501 ± 0.012	0.377 ± 0.012	0.621 ± 0.022
12 + log(O/H)	7.796 ± 0.012	7.696 ± 0.014	7.700 ± 0.011	7.576 ± 0.014	7.793 ± 0.015
N^+/H^+ ($\times10^6$)	0.232 ± 0.011	0.187 ± 0.012	0.173 ± 0.005	0.079 ± 0.012	0.055 ± 0.010
ICF	7.691	11.401	8.151	17.253	22.543
log(N/O)	−1.544 ± 0.026	−1.368 ± 0.032	−1.551 ± 0.018	−1.440 ± 0.073	−1.701 ± 0.087
Ne^{++}/H^+ ($\times10^5$)	1.045 ± 0.037	0.806 ± 0.031	0.840 ± 0.025	0.636 ± 0.023	1.271 ± 0.050
ICF	1.046	1.040	1.044	1.028	1.025

Table 7. continued.

	Galaxy				
log(Ne/O)	−0.757 ± 0.021	−0.773 ± 0.023	−0.757 ± 0.018	−0.761 ± 0.022	−0.678 ± 0.024
S^+/H^+ ($\times10^6$)	0.118 ± 0.003	0.085 ± 0.003	0.100 ± 0.002	0.041 ± 0.003	0.035 ± 0.005
S^{++}/H^+ ($\times10^6$)	0.784 ± 0.061	0.805 ± 0.072	0.716 ± 0.039	0.252 ± 0.045	...
ICF	1.791	2.402	1.866	3.375	...
log(S/O)	−1.588 ± 0.032	−1.367 ± 0.038	−1.518 ± 0.023	−1.582 ± 0.068	...
Cl^{++}/H^+ ($\times10^8$)	...	...	...	...	...
ICF	...	...	...	...	...
log(Cl/O)	...	...	...	...	...
Ar^{++}/H^+ ($\times10^7$)	2.377 ± 0.088	1.829 ± 0.107	1.774 ± 0.055	0.957 ± 0.085	0.927 ± 0.103
Ar^{+++}/H^+ ($\times10^7$)	0.793 ± 0.089	1.137 ± 0.129	1.084 ± 0.072	1.455 ± 0.094	2.176 ± 0.167
ICF	1.715	2.318	1.788	3.300	4.197
log(Ar/O)	−2.186 ± 0.026	−2.069 ± 0.042	−2.199 ± 0.024	−2.077 ± 0.059	−2.203 ± 0.093
$Fe^{++}/H^+(\times10^6)$(4658)	0.125 ± 0.024	0.225 ± 0.028	0.143 ± 0.020	...	...
$Fe^{++}/H^+(\times10^6)$(4988)	0.255 ± 0.031	...	...	...	...
ICF	11.156	16.938	11.871	...	...
log(Fe/O) (λ4658)	−1.651 ± 0.083	−1.116 ± 0.056	−1.470 ± 0.062	...	...
log(Fe/O) (4988)	−1.342 ± 0.054	...	...	...	...

[a] Direct method.

Table 8. Ionic and total heavy element abundances derived from the high-resolution MMT spectra.

	Galaxy				
Property	J0810+1837[a]	J0833+2508 No.1[a]	J0833+2508 No.2[a]	J0931+2717 No.1[b]	J0931+2717 No.2[b]
T_e(O III) (K)	14517 ± 3643	15635 ± 820	21239 ± 4080	17809 ± 1015	17147 ± 1014
T_e(O II) (K)	13945 ± 3212	14661 ± 702	16405 ± 2740	15702 ± 1241	15434 ± 1226
O^+/H^+ ($\times10^4$)	0.381 ± 0.247	0.210 ± 0.027	0.172 ± 0.069	0.175 ± 0.035	0.199 ± 0.041
O^{++}/H^+ ($\times10^4$)	0.292 ± 0.193	0.281 ± 0.038	0.100 ± 0.042	0.106 ± 0.015	0.134 ± 0.020
O^{+++}/H^+ ($\times10^6$)	...	...	...	...	...
O/H ($\times10^4$)	0.673 ± 0.314	0.491 ± 0.046	0.272 ± 0.081	0.281 ± 0.038	0.333 ± 0.045
12 + log(O/H)	7.828 ± 0.202	7.691 ± 0.041	7.434 ± 0.130	7.448 ± 0.059	7.522 ± 0.059
Ne^{++}/H^+ ($\times10^5$)	0.781 ± 0.550	0.544 ± 0.078	0.346 ± 0.140	0.210 ± 0.050	0.253 ± 0.063
ICF	1.258	1.171	1.304	1.298	1.280
log(Ne/O)	−0.836 ± 0.597	−0.887 ± 0.102	−0.780 ± 0.390	−1.012 ± 0.218	−1.012 ± 0.220
Property	DDO68 No.3[a]	DDO68 No.4[a]	J1057+1358 No.1[b]	J1121+3744 No.1[b]	J1231+4205[a]
T_e(O III) (K)	16721 ± 747	16521 ± 1935	20000 ± 1061	20000 ± 1066	15730 ± 761
T_e(O II) (K)	15239 ± 618	15141 ± 1610	16284 ± 1345	16284 ± 1351	14716 ± 649
O^+/H^+ ($\times10^4$)	0.044 ± 0.005	0.083 ± 0.023	0.119 ± 0.025	0.061 ± 0.014	0.209 ± 0.025
O^{++}/H^+ ($\times10^4$)	0.098 ± 0.011	0.060 ± 0.017	0.034 ± 0.005	0.069 ± 0.010	0.208 ± 0.026
O^{+++}/H^+ ($\times10^6$)	...	...	...	...	...
O/H ($\times10^4$)	0.142 ± 0.012	0.143 ± 0.029	0.152 ± 0.026	0.130 ± 0.017	0.418 ± 0.036
12 + log(O/H)	7.152 ± 0.036	7.155 ± 0.087	7.182 ± 0.073	7.115 ± 0.057	7.621 ± 0.037
Ne^{++}/H^+ ($\times10^5$)	0.199 ± 0.023	0.135 ± 0.040	...	...	0.459 ± 0.061
ICF	1.110	1.267	...	...	1.215
log(Ne/O)	−0.808 ± 0.074	−0.924 ± 0.259	...	...	−0.875 ± 0.103
Property	J0834+5905[a]	J0959+4626[b]			
T_e(O III) (K)	21493 ± 2679	17404 ± 1007			
T_e(O II) (K)	16411 ± 1769	15543 ± 1223			
O^+/H^+ ($\times10^4$)	0.092 ± 0.024	0.216 ± 0.043			
O^{++}/H^+ ($\times10^4$)	0.082 ± 0.022	0.103 ± 0.014			
O^{+++}/H^+ ($\times10^6$)	...	...			
O/H ($\times10^4$)	0.174 ± 0.033	0.319 ± 0.046			
12 + log(O/H)	7.241 ± 0.082	7.504 ± 0.062			
Ne^{++}/H^+ ($\times10^5$)	0.183 ± 0.052	0.292 ± 0.061			
ICF	1.233	1.339			
log(Ne/O)	−0.887 ± 0.228	−0.912 ± 0.219			

[a] Direct method. [b] Semi-empirical method.

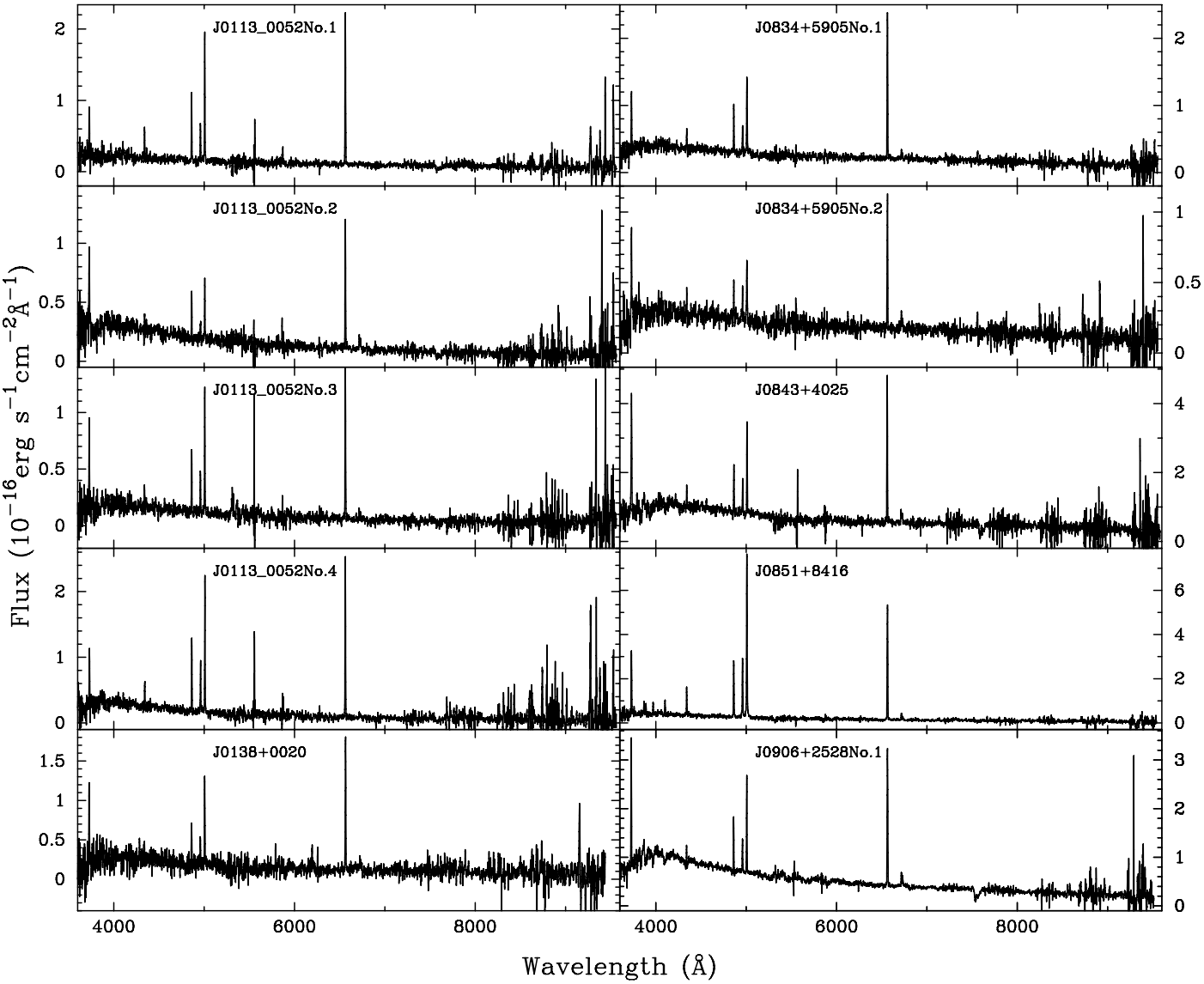

Fig. 1. 3.5 m APO spectra of galaxies.

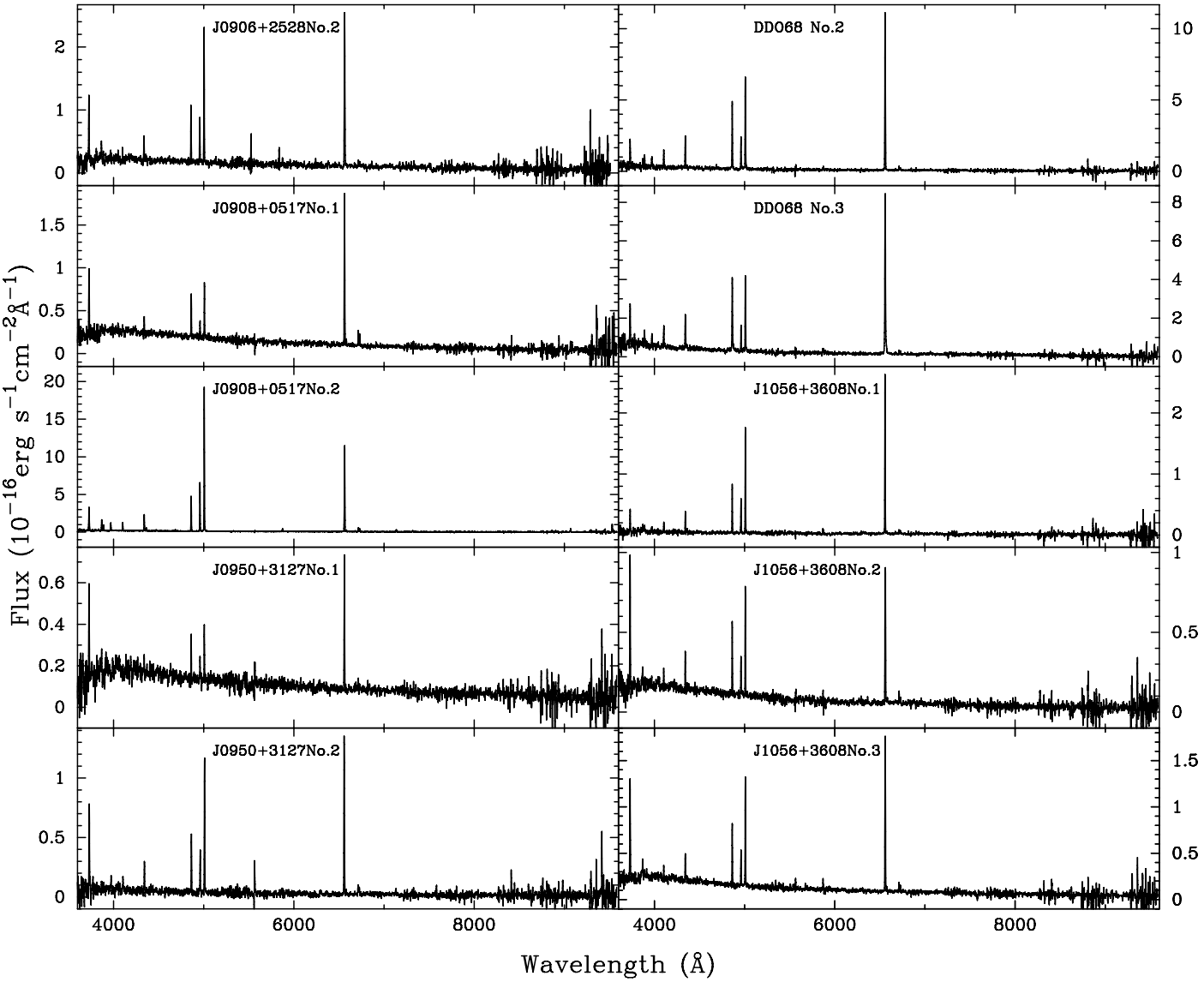

Fig. 1. continued.

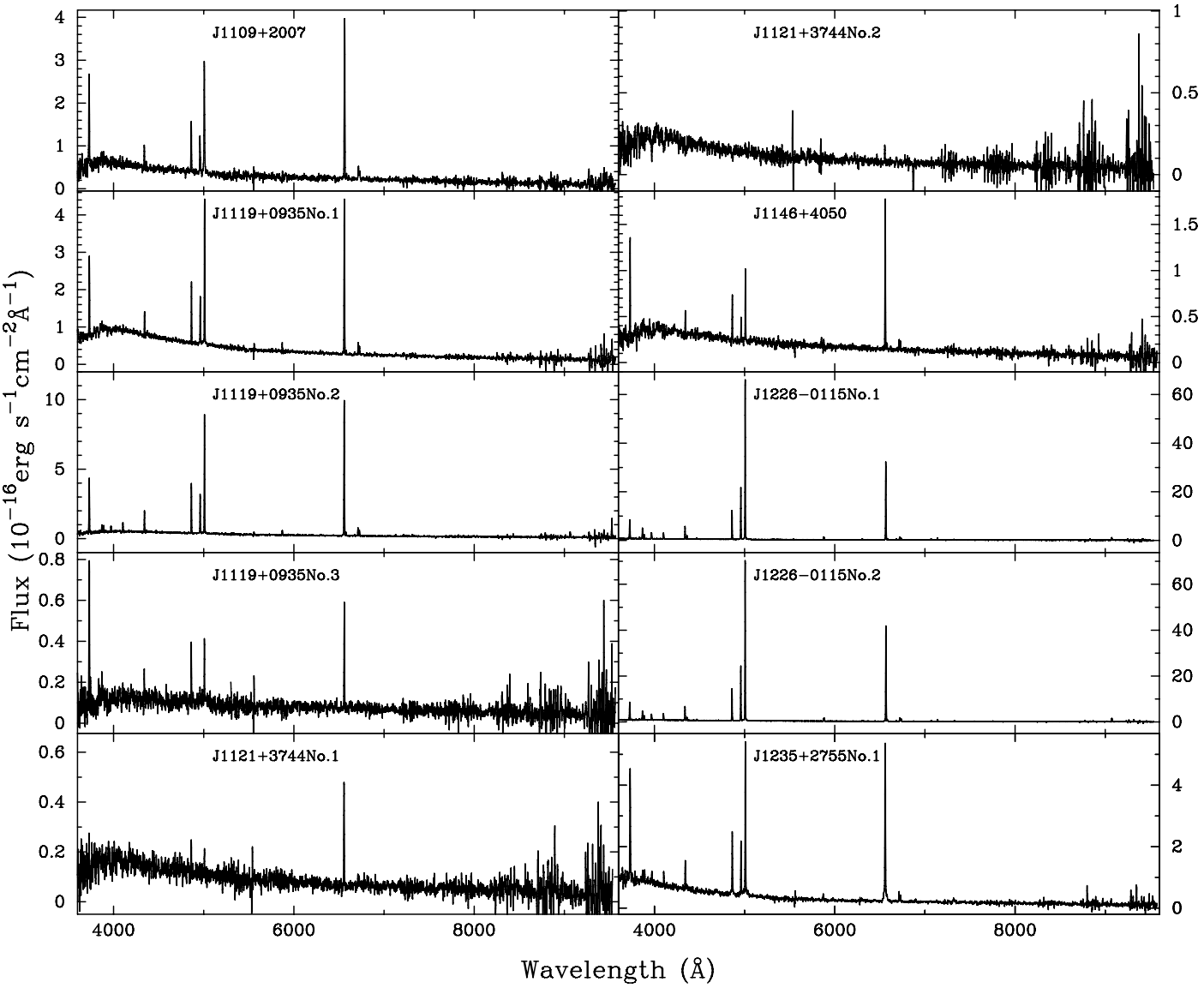

Fig. 1. continued.

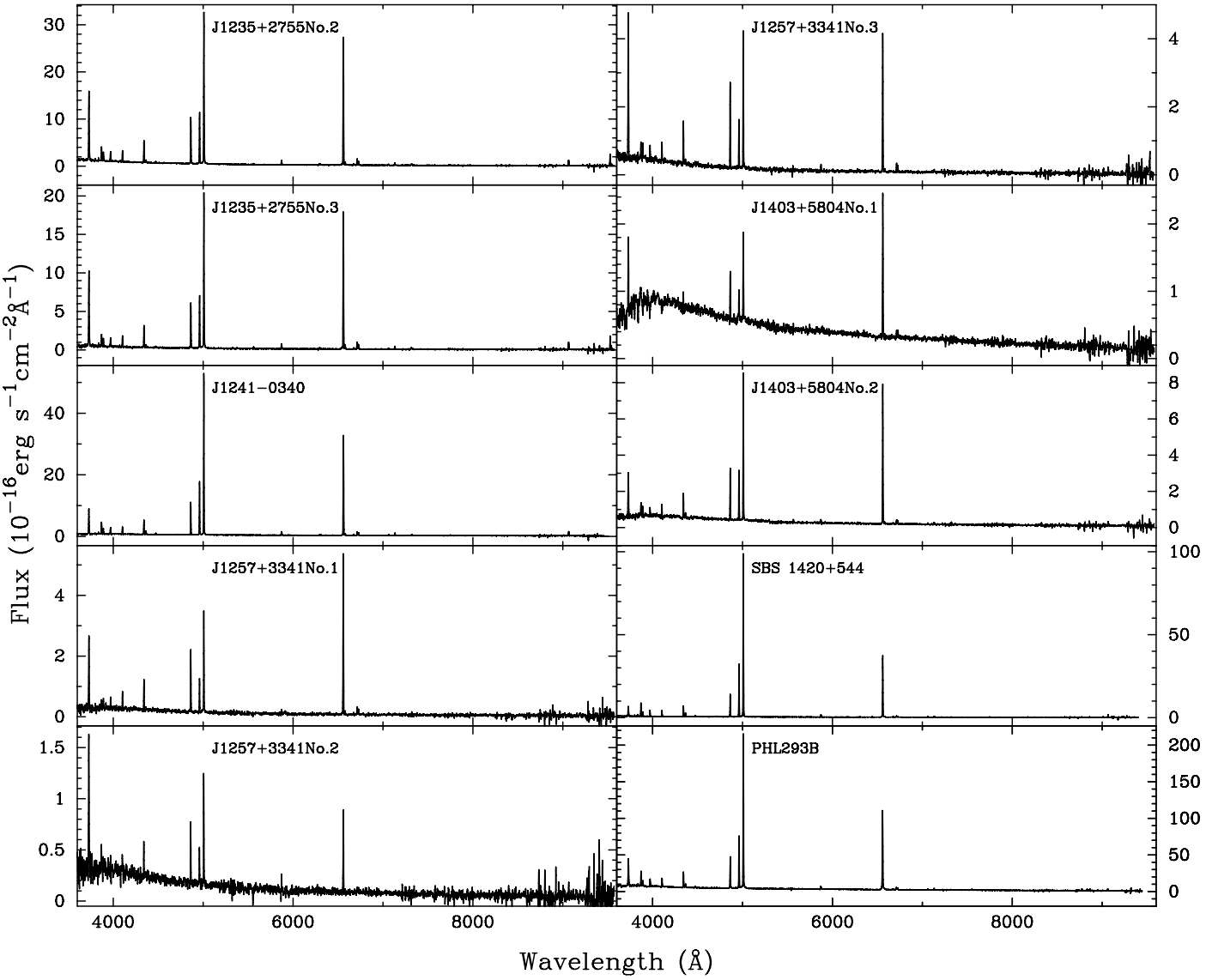

Fig. 1. continued.

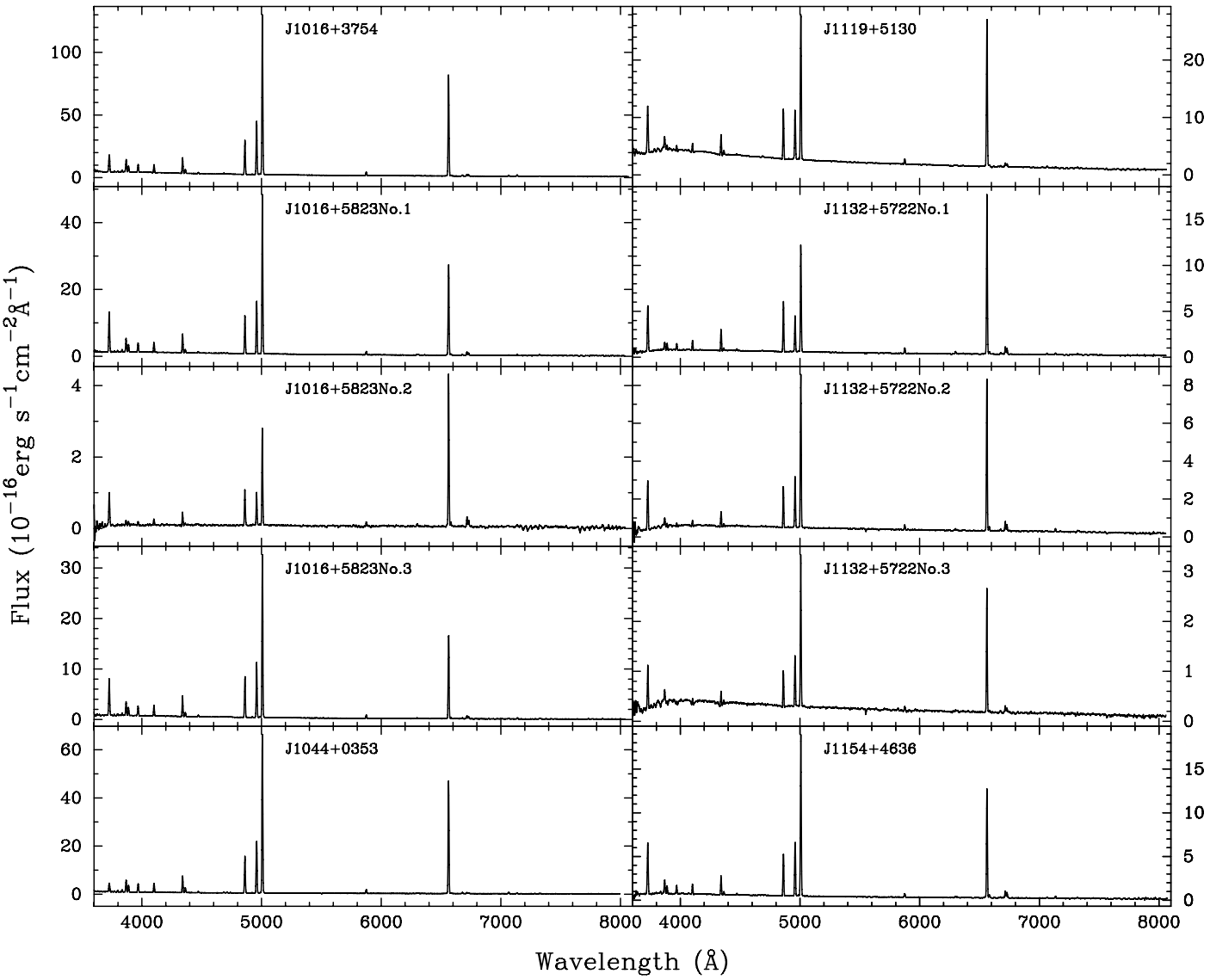

Fig. 2. Low-resolution MMT spectra.

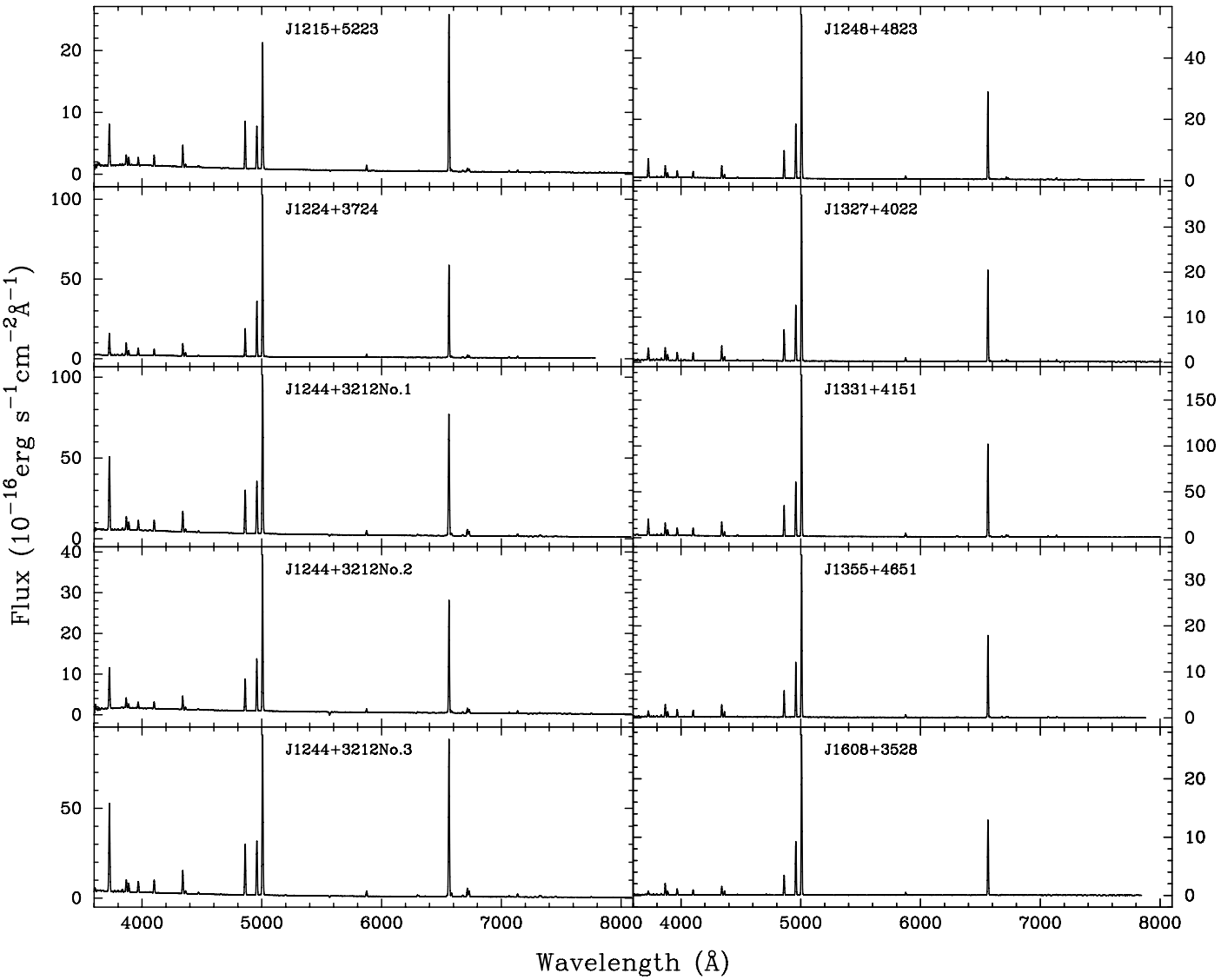

Fig. 2. continued.

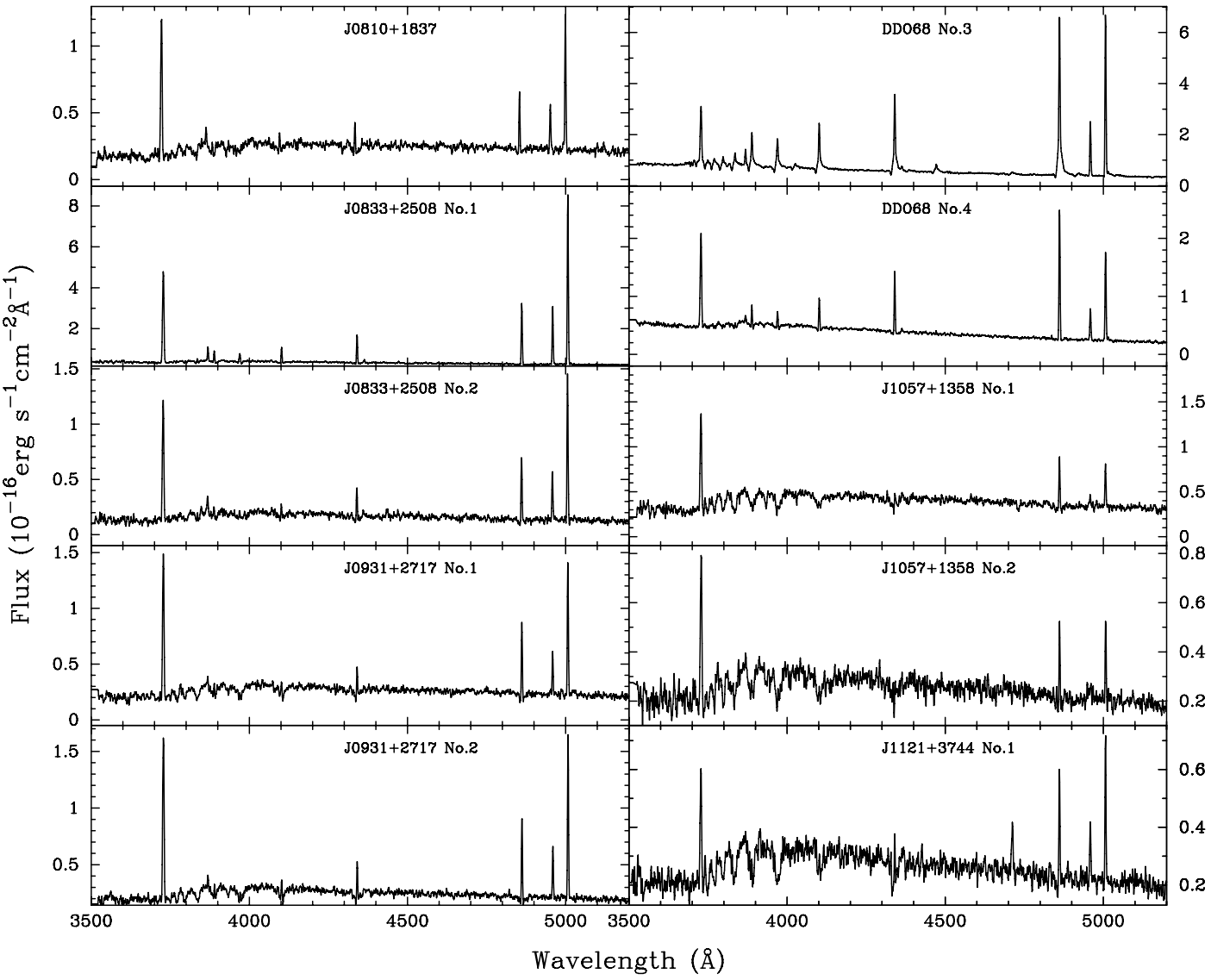

Fig. 3. Medium-resolution MMT spectra.

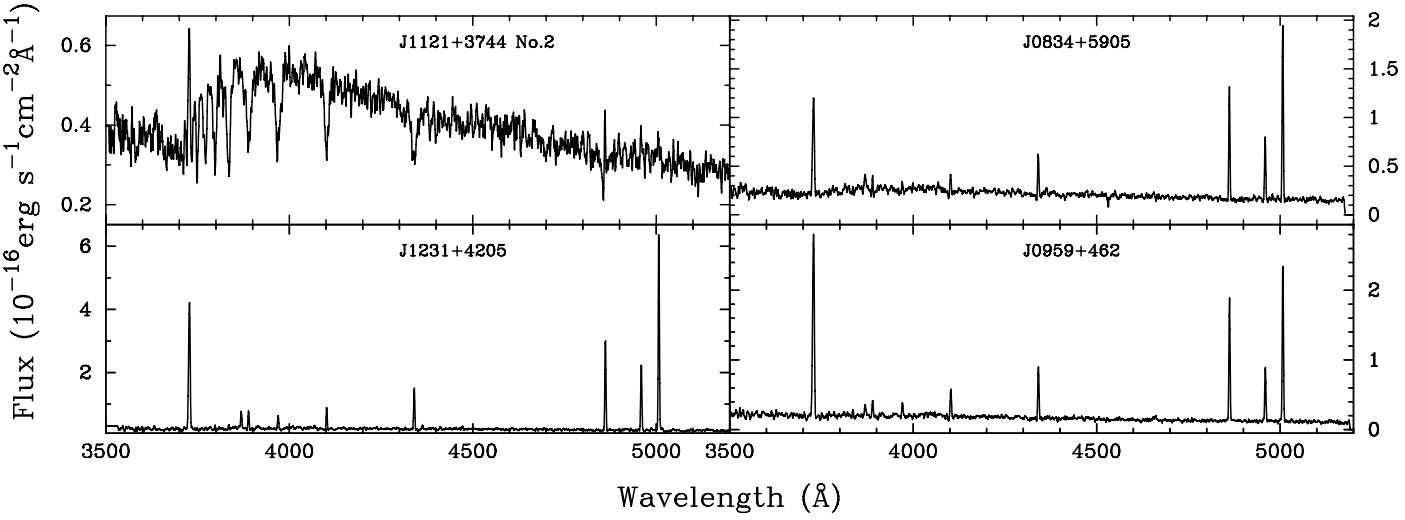

Fig. 3. continued.